U.S. DEPARTMENT OF ENERGY

Office of ENERGY EFFICIENCY & RENEWABLE ENERGY

Investigation of the Long-Term Aging Characteristics of Chip-On-Board LEDs: Initial Benchmarks

U.S. Department of Energy—Lighting R&D Program

September 2021

(This page intentionally left blank)

RTI Project Number
0215939.001.001

Investigation of the Long-Term Aging Characteristics of Chip-on-Board LEDs: Initial Benchmarks

September 2021

Prepared for

U.S. Department of Energy

Through contract with
KeyLogic Systems, Inc.
3168 Collins Ferry Road
Morgantown, WV 26505

Prepared by

J. Lynn Davis, Kelley Rountree, Roger Pope,
Michelle McCombs, Meghan Hegarty-Craver, and Karmann Mills
RTI International
3040 E. Cornwallis Road
Research Triangle Park, NC 27709

Acknowledgments

This material is based upon work supported by the U.S. Department of Energy's Office of Energy Efficiency and Renewable Energy (EERE) under the National Energy Technology Laboratory (NETL) Mission Execution and Strategic Analysis (MESA) contract, award number DE-FE0025912.

Disclaimer

Nomenclature or List of Acronyms

45OL	operational life test conducted at 45°C
75OL	operational life test conducted at 75°C
α	decay rate constant in the ANSI/IES TM-21-2019 model
$\Delta u'$	change in the u' coordinate of chromaticity
$\Delta u'v'$	chromaticity shift magnitude or the total change in chromaticity coordinates
$\Delta v'$	change in the v' coordinate of chromaticity
$\eta_{LED,EQE}$	external quantum efficiency of an LED
Θ_{cs}	thermal resistance between the LED case and the heat sink
Θ_{sa}	thermal resistance between the heat sink and ambient air
$\lambda_{LED,max}$	LED maximum emission wavelength
$\lambda_{phos,max}$	phosphor maximum emission wavelength
v	emission frequency
$\Phi(t)$	luminous flux at time t
Φ_0	initial luminous flux
Φ_e	radiant flux
°C	degree Celsius
°C/W	degrees Celsius per watt
°C-m/W	degrees Celsius meter per watt
Ag	silver
Al_2O_3	aluminum oxide or alumina
AlN	aluminum nitride
ANSI	American National Standards Institute
AST	accelerated stress test
Au	gold
B	projected initial constant in TM-21-19
b	y-axis intercept of the CCT value, also known as the projected initial CCT value
CCT	correlated color temperature
$CCT(t)$	CCT value at time, t

CIE	International Commission on Illumination (*Commission Internationale de l'Éclairage*)
cm	centimeter
cm^2	square centimeter
COB	chip-on-board
CRI	color rendering index
CSM	chromaticity shift mode
CSP	chip-scale package
Cu	copper
dc	direct current
DOE	U.S. Department of Energy
DUT	device under test
e	electron charge
EERE	Office of Energy Efficiency and Renewable Energy
EQE	external quantum efficiency
g	gram
GaN	gallium nitride
HP-LED	high-power LED
h	Planck's constant
hr, hrs	hour, hours
hv	photon energy at the emission frequency, v
I	injection current
IES	Illuminating Engineering Society
I_f	forward current
K	Kelvin
LED	light-emitting diode
LES	light-emitting surface
LFM	luminous flux maintenance
lm	lumen

lm/W	lumens per watt
m	slope or change in the CCT value with time (i.e., $\Delta y/\Delta t$)
mA	milliampere
mA/cm^2	milliamperes per square centimeter
MCPCB	metal-core printed circuit board
MESA	Mission Execution and Strategic Analysis
min	minute
mm	millimeter
MP-LED	mid-power LED
MS	modified spectrum, modified spectra
NETL	National Energy Technology Laboratory
NIST	National Institute of Standards and Technology
nm	nanometer
PCB	printed circuit board
pc-LED	phosphor-converted LED
R^2	correlation coefficient
R_f	color fidelity index in ANSI/IES TM-30-18
R_g	color gamut index in ANSI/IES TM-30-18
RTOL	room temperature operating life
sec	second
SPD	spectral power distribution
SSL	solid-state lighting
t	time
T_c	case temperature
TIM	thermal interface material
T_j	junction temperature
TM	technical memorandum
u'	chromaticity coordinate in the CIE 1976 color space
$u'(t)$	u' chromaticity coordinate measured at time, t

u'_0	initial value of the v' chromaticity coordinate
V	volt
v'	chromaticity coordinate in the CIE 1976 color space
V_f	forward voltage
$v'(t)$	v' chromaticity coordinate measured at time, t
v'_0	initial value of the v' chromaticity coordinate
W	watt

Executive Summary

There are four main classes of light-emitting diode (LED) package platforms that are currently used in solid-state lighting (SSL) technologies. These classes of packaging platforms are high-power light-emitting diodes (HP-LEDs), mid-power LEDs (MP-LEDs), chip-scale package (CSP) LEDs, and chip-on-board (COB) LEDs. Each MP-LED, HP-LED, and CSP LED package typically has only one to three LED die that are energized through two electrodes (i.e., an anode and a cathode). In contrast, COB LED packages can contain many more LED die in a single package, but still are energized through only two electrodes. As a result of the inherent high LED die count, the COB LED package platform offers the highest lighting flux density available in a thin, low-profile package. For example, it is possible to produce several thousand lumens (lm) from the light-emitting surface (LES) of a COB LED that occupies as little as 0.25 square inches (1.6 square centimeters [cm]). COB LEDs achieve this level of performance by integrating many MP-LED die into the LES and electrically connecting them through wire bond or solder interconnects. The LED array is directly mounted on an excellent thermal conductor such as a metal-core printed circuit board (MCPCB) or a ceramic substrate to manage the waste heat. COB LED packages are typically set to a fixed correlated color temperature (CCT) value. Some advanced COB LED packages can contain two or more LED primaries set to different CCT values and can be tuned between the CCT values of the LED primaries by adjusting the current to each. The COB LED package for such products contains separate electrodes for each LED primary to allow tunable-white operation.

The first SSL products typically used either HP-LEDs or MP-LEDs. Each of these packaging platforms were found to have particular mechanisms related to the LED package that caused either luminous flux depreciation or chromaticity shift. Because a decade of laboratory research and field performance data have been collected, analyzed, and are available, the degradation mechanisms of HP-LEDs and MP-LEDs are better understood today than in the early days of SSL products. However, COB LEDs are a relatively new LED packaging technology; therefore, the failure mechanisms specific to this LED package platform are not as well understood. The primary failure mechanisms associated with COB LEDs are thought to arise from two driving factors—the amount of heat generated in the COB LED package and the large area of silicone in the package, which can lead to moisture ingress.

This report is the first in a series of reports about the reliability of commercial COB LED products; therefore, it will focus specifically on thermal issues in COB LEDs. In this report, reliability is judged by either lights-out failures caused by electrical open circuits or parametric failures caused by excessive luminous flux depreciation or chromaticity shifts. Six different COB LED products from different Tier 1 manufacturers were included in this study. All of the COB LEDs were phosphor-converted LEDs (pc-LEDs), and the LES of the devices under test (DUTs) varied from 4.5 millimeters (mm) to 14.6 mm. Most DUTs were set to a fixed CCT value, but the CCT values of two classes of DUTs were tunable; therefore, this study offers new insights into the behavior of this type of LED products.

The initial part of this study consisted of a comparison of the construction techniques used in the different DUTs. Four out of the six classes of DUTs examined during this study were built on MCPCBs, with the remaining two classes of DUTs being built on ceramic substrates. Five out of the six classes of DUTs contained LED die that were interconnected by wire bonding, and the LED die in these products were mounted to the substrate with a thermally conductive adhesive. The LED die in the sixth class of DUTs were flip-chip bonded to an interposer layer on the aluminum nitride (AlN) substrate through solder bumps. The number of LEDs in the LES ranged from 12 (for a 4.5-mm LES) to 108 (for a 14.6-mm LED). The radiant efficiency of these devices ranged from 0.31 to 0.44, and the luminous efficacy of these samples ranged from 83 lumens per watt (lm/W) to 127 lm/W.

Because the LED die used in COB LED packages are similar in size to those used in MP-LEDs, a tunable-white MP-LED product was chosen for comparison purposes. The tunable-white MP-LED DUTs contained two independent circuits of one LED die each, with one circuit tuned to a nominal CCT value of 2,700 Kelvin

(K) and the other circuit tuned to a nominal CCT value of 6,500 K. The MP-LED DUTs had the two LED die bonded on a silver lead frame and connected via wire bonds. As a whole, this structure is analogous to many of the COB LEDs examined during this study, but it operates at a lower power level and produces less waste heat. The MP-LED product was found to be more efficient than any of the COB LED products with radiant efficiency of the MP-LED product between 0.47 and 0.52 (depending on the CCT value), and luminous efficacies between 152 lm/W to 162 lm/W (depending on CCT value). The authors of this report attribute the higher efficiency of the MP-LED package to the smaller amount of waste thermal energy that must be dissipated and the smaller number of absorbing surfaces (e.g., other LED die, wire bonds) in the MP-LED package compared with the COB LED package.

Prior to testing the COB LED DUTs, the samples were mounted on appropriate heat sinks intended to keep the case temperature (T_c) of the COB LED package within the manufacturer's specifications. Room temperature operating life (RTOL) tests were conducted on these COB LED DUTs (mounted to a heat sink by using a silicone thermal grease as a thermal interface material [TIM]) in still air, and the T_c values varied between 69 degrees Celsius (°C) and 113°C. The luminous flux maintenance (LFM) data were analyzed by using an exponential decay model as indicated in the American National Standards Institute (ANSI) and Illuminating Engineering Society (IES) technical memorandum (TM) ANSI/IES TM-21-19. The LFM values in RTOL for many DUTs increased during the first 6,000 hours (hrs) of operation, indicating an improvement in efficiency, and they were assigned a decay rate constant (α) value of 2.0×10^{-6} as required by ANSI/IES TM-21-19. Minimal chromaticity shift was observed for the devices during RTOL tests. Therefore, neither "lights out" nor parametric failures were observed through 6,000 hrs of the RTOL tests.

Separate populations of some of the DUTs were also operated in elevated ambient environment of 75°C, during 75°C operational life (75OL) tests in an environmental chamber with high air circulation. The 75OL tests proved to be a higher stress environment that produced α values significantly higher than those measured in RTOL tests even though the T_c values were not that different. The reason for the higher stress levels in 75OL is not clear since the T_c values are expected to be similar in 75OL (with high air recirculation) and RTOL (with no forced air circulation). One possible cause of this difference in α values was a change in the thermal resistance of at least one interface (e.g., the TIM) over time because of degradation, but this could not be confirmed experimentally. The 75OL condition did accelerate luminous flux depreciation, but all DUTs exhibited LFM values well above the parametric failure threshold (i.e., LFM $\leq$ 0.7) during the 6,000-hr test duration. In addition, the chromaticity shifts of the COB LED DUTs during the 75OL test were similar to those observed during the RTOL test, but the magnitude of the shifts was greater in 75OL. As a result, parametric failure because of excessive chromaticity shift (i.e., $\Delta u'v' \leq 0.007$) occurred for some DUTs in 75OL but not all.

All DUTs examined during this study exhibited either shifts in the blue or green direction or a combination of the two during the test period; either shift is indicative of chromaticity shift mode (CSM) behavior that can be classified as CSM-1 or CSM-2. CSM-1 is usually caused by a relative increase in emissions from the LED emitter, whereas CSM-2 is usually caused by a change in the emission spectrum of warm white phosphors. In keeping with these previous findings, CSM-1 behavior was observed exclusively for the cool white DUTs examined during this study; in contrast, many of the 2,700 K DUTs included in this report exhibited mostly CSM-2 behavior. In some instances, both CSM-1 and CSM-2 behaviors were observed simultaneously, which suggests that both CSMs may be active. No DUTs evaluated during the RTOL test exhibited a chromaticity shift that exceeded the normal parametric thresholds from chromaticity shift failure (e.g., $\Delta u'v' = 0.007$, $\Delta u'v' = 0.004$), but both the neutral white and cool white settings of the tunable COB product can be classified as parametric failures because of excess chromaticity shift during the 75OL test.

In order to understand the performance of the LEDs used in the mid-power package, several of the product types investigated in this report were decapped to remove the silicone and phosphor layer. The decapping results indicated that the external quantum efficiencies (EQE) of the COB LEDs ranged between 0.46 and 0.67. This lowest EQE value, 0.46, was observed for a violet-pumped COB LED, and the reduced EQE value may be related to the LED epitaxy or the alumina (Al_2O_3) substrate. The best performing COB LED product had a EQE of 0.67 and was the only flip-chip bonded product examined during this study. The performance of the flip-chip COB LED product was similar to that of the MP-LED package that was used as the benchmark, which had an EQE of 0.66.

COB LEDs are an emerging LED packaging platform for SSL products that offers products in high lighting density and in a thin profile. Recent advances in packaging of COB LED products have also provided tunable light capabilities in this package platform either as a dim-to-warm product or as a white-tunable product. However, this initial report underscores the importance of thermal management with COB LED technologies because of the high density of waste heat that is generated by the small package. During room temperature testing, where the T_c was properly controlled, the luminous flux maintenance performance of the COB LED products was excellent, with most decay rate constants calculated to be at the minimum value allowed by ANSI/IES TM-21-19. COB LED packages offer new capabilities to the SSL industry in a denser package than those offered by other platforms. The high light density in a thin profile may help to create new SSL products with advanced lighting features such as tunable white or unique optical patterns for light delivery. The key to capitalizing on these new capabilities is proper design of the luminous containing the COB LED, especially the thermal management pathways.

Table of Contents

List of Figures

List of Tables

1 Introduction

Chip-on-board (COB) light-emitting diodes (LEDs) are a relatively new LED package platform. The package consists of an array of interconnected LED die placed on a low thermal resistance substrate. The assembly is covered by a large phosphor-silicone layer creating a phosphor-converted LED (pc-LED), which gives this LED package platform the appearance of a "fried egg." Representative examples of COB LEDs are shown in **Figure 1-1**. The LEDs used in the COB LED package platform are similar in size and current density to those used in mid-power LED (MP-LED) and chip-scale package (CSP) LED platforms, but the numbers of LEDs used in the COB LED packaging platform are much higher, producing more light but also producing more waste heat per unit area. Even though there are many LED die in a COB LED package, there is typically only one set of electrodes—an anode and a cathode. The LED die in the COB LED package are connected in various series and parallel combinations that result in higher forward voltages (V_f) and forward currents (I_f) being required to operate a COB LED package than those required for single-die LED packages. It is not uncommon for the drive voltage of a COB LED to be between 20 volts (V) and 50 V, with I_f values between 300 milliamperes (mA) and greater than 4,000 mA for large light-emitting surface (LES) devices. Another key difference between the MP-LED and COB LED packaging platforms is that, in MP-LEDs, the LEDs are bonded to a lead frame, which is then encased in a polymer package. In contrast, in COB LEDs, the LED die are bonded directly to the exterior package (i.e., the substrate) to lower thermal impedance and improve heat management. As a result, the COB LED package platform offers the highest lighting density that is available from a low-profile LES. There are two main architectures for the COB LED package platform: one using a metal-core printed circuit board (MCPCB) substrate and the other using a ceramic substrate.

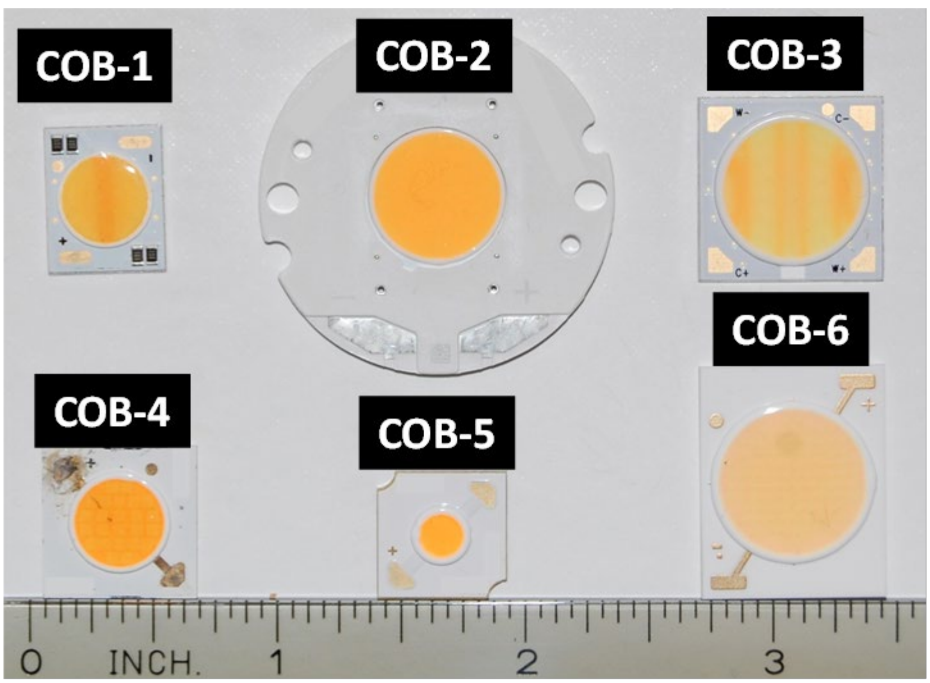

Figure 1-1: Examples of the COB LED packages examined during this study.

The major components of a COB LED package built on an MCPCB substrate are shown in **Figure 1-2**. The metal core is typically made from aluminum with a smooth reflective surface on one side, usually a silver (Ag) thin film, that will serve as the substrate for mounting the LEDs and the conduit for heat dissipation. A polymer dielectric material is applied to the substrate with a conductive copper (Cu) layer attached to the top of the dielectric. This dielectric can range from a thin FR-4 printed circuit board (PCB) laminate to a polymer film. The Cu layer is imaged and etched to form the electrode headers and conductor patterns, and a photoimageable white polymer solder mask is applied on top of the etched Cu. After photoimaging, the solder mask is processed to expose the electrical header in the middle of the COB LED package, and the exposed metal undergoes electroplating to build conductor thickness. The electroplating process typically ends with a thin barrier layer (e.g., nickel) being electroplated on top of the Cu conductor, and a gold (Au) layer is electroplated as a finishing step. The purpose of the thin barrier layer is to prevent Cu and Au interdiffusion, which can impact the ability to successfully wire bond and solder to the metallization. The purpose of the Au layer is to promote both good wire bonding and soldering on the surface of the conductor. Then, the LED die are attached to the substrate, typically by using a thermally conductive adhesive, and the array is wire bonded in various series-parallel combinations. The image shown in **Figure 1-2** has two parallel strings of six LEDs in series (i.e., LED array 1 and LED array 2) for a total of 12 LEDs. After wire bonding has been completed, a dam for the phosphor-silicone material is created by dispensing a viscous silicone material on the electrode header. This silicone perimeter serves two functions: (1) containing the phosphor-silicone layer and (2) protecting the wire bonds attached to the electrode header. Once curing of the dam has been completed, the phosphor-silicone mixture can be dispensed or printed over the LEDs to complete the assembly.

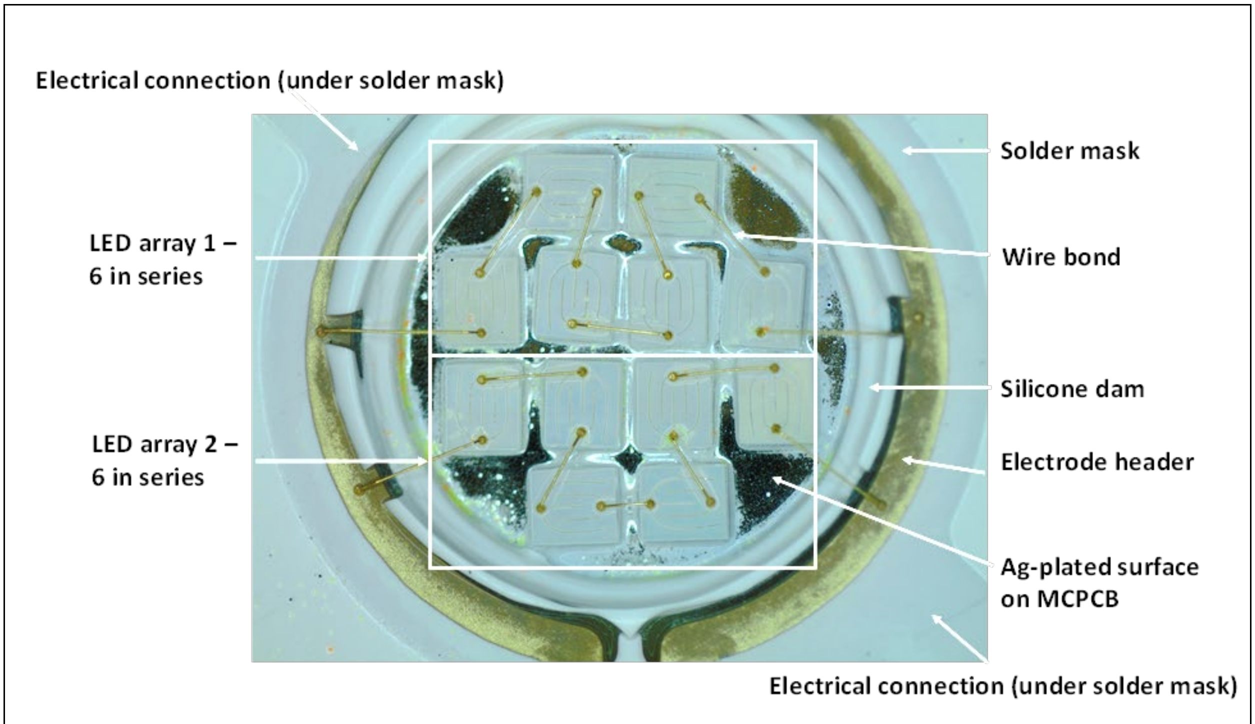

Figure 1-2: The major components of a COB LED package made on an MCPCB substrate.

The major components of a COB LED package built on a ceramic substate are shown in **Figure 1-3**. The most widely used ceramic substrate for this architecture is aluminum oxide (Al_2O_3) (also known as alumina), although aluminum nitride (AlN), which has a higher thermal conductivity, can also be used. The ceramic substrate is typically made from a fired ceramic plate. Because the visible light reflectance of AlN is low, a thin white polymer dielectric may be placed on top of the AlN. Then, the ceramic plate (or polymer film if present) is metallized either by applying conductive inks as thick films through a screen or sputter coating metal on the substrate. When thin film metallization (e.g., sputtering) is employed, additional process steps (e.g., photolithograph, electroplating) are used to create the conductor. The resulting substrates contain the electrical leads, the electrode header, and the die bond pads on the monolithic substate. Then, the LED die are attached to the die bond pads on the substrate usually with solder bonds (for flip-chip interconnections as in

Figure 1-3) or conductive epoxy adhesives for wire bond interconnections. It is typical for the LEDs in the ceramic substrate architecture to have various series-parallel combinations of LEDs. The image shown in **Figure 1-3** has two parallel strings of 12 LEDs in series (labeled 1 through 12 in yellow and red, respectively) for a total of 24 LEDs. After the bonding and chip-to-chip interconnection has been completed, a dam for the phosphor-silicone material is created by dispensing a viscous material onto the electrode header. This silicone perimeter serves two functions: (1) containing the phosphor-silicone layer and (2) protecting the electrode header from damage or corrosion. Once curing of the dam has been completed, the phosphor-silicone mixture can be dispensed or printed over the LEDs to complete the assembly.

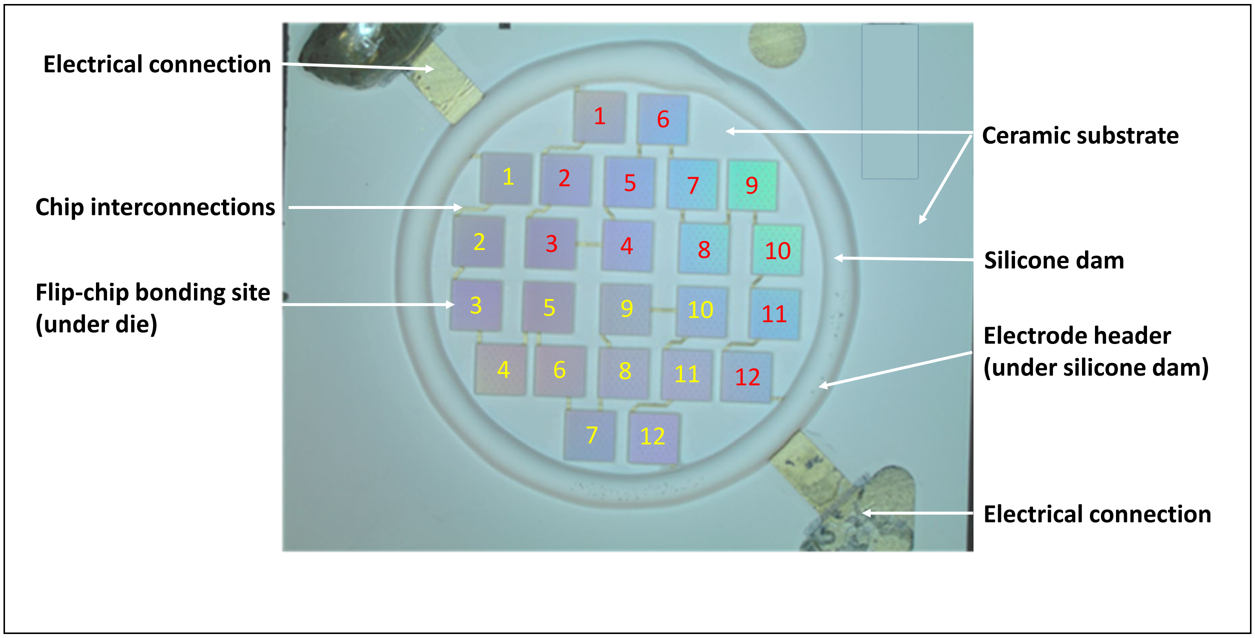

Figure 1-3: The major components of a COB LED package made from a ceramic substrate.

Although the COB LED package platform can produce high luminous flux densities, it is typically not as efficacious as the MP-LED and CSP LED package platforms. This is partly due to the large number of die and interconnects within the LES of a typical COB, and these surfaces are potential points of light absorption. In addition, the high density of waste heat generated in some COB LED packages can also affect the luminous efficacy during use. As a result, COB LED packages can offer luminous efficacies of more than 100 lumens per watt (lm/W), but these values are typically 20% or more below what can be achieved in MP-LEDs [1]. Although the initial luminous efficacies of COB LEDs are typically lower than that of other LED package platforms, the luminous flux maintenance (LFM) and chromaticity maintenance are typically higher. These higher values are because the materials used in the COB LEDs (e.g., metal, ceramic) are typically more stable than some of the packaging materials employed in other LED package platforms (e.g., polymer resins) [2]. The primary causes of poor luminous flux or chromaticity maintenance in COB LED packages are typically linked to thermal management issues and preventing moisture ingress through the large silicone surface area [1]. The thermal management properties of COB LEDs depend on the spacing of the LEDs in the array, the thermal resistance between the LED junctions and the heat sink, and whether active cooling (e.g., water, forced air) are used [3].

The correlated color temperature (CCT) of COB LEDs is determined by the phosphor-silicone mix that is placed over the LED array, and there are several options available in commercial products. Most COB LEDs are set to a fixed CCT value. Some examples of these types of product include Products COB-2, COB-4, COB-5, and COB-6 which have LESs of uniform colors as shown in **Figure 1-1**. By placing different phosphor mixes over different LEDs in the COB LED array, dim-to-warm and tunable-white COB LED products can be made. Product COB-1 in **Figure 1-1** is a dim-to-warm COB LED package with the dim emissions (CCT of 1,800 Kelvin [K]) occurring from a dark orange strip in the middle of the LES and the warm white (CCT of 3,000 K) occurring from the LES as a whole. The CCT value of Product COB-1 can be varied between 1,800 K and 3,000 K based solely on the current and voltage provided to the two electrodes. This dim-to-warm lighting technology has been previously reviewed [4,5]. Tunable-white COB LEDs with CCT values that can be tuned linearly between two endpoints are made by placing a warm white phosphor (i.e., orange stripes for Product COB-3 in **Figure 1-1**) over half of the LEDs and a cool white phosphor (i.e., yellow stripes in **Figure 1-1**) over the remaining LEDs. Because the two LED arrays are operated independently (i.e., separate anodes and cathodes are present for each string), the devices can be tuned across the CCT range (e.g., 2,700 K to 6,500 K) by independently adjusting the I_f value supplied to each array. As a result, there are four electrical leads on a tunable-white COB LED package: one anode and cathode set for the warm white array and another set for the cool white array.

Because of the high luminous flux densities and optical uniformities that are available from the LES of a typical COB, these devices are often used in applications such as street lighting, spot lighting, and high bays that require high-power sources. The annual sales of COB LED products are approximately $14 billion, and this segment of the LED lighting industry is growing at a healthy compound growth rate of 12% annually [6]. One of the biggest advantages of using COB LEDs is the ease of integration into a finished product because only two electrical leads are required to connect to the luminaire. In addition, new capabilities imparted by COB LEDs to SSL devices such as tunable-white features and small source size will help to create new products that will further accelerate the growth of COB lighting.

In 2018, the cost breakdown of a 20-watt (W) MCPCB COB LED was as follows:

- Assembly costs: 43%
- Die costs: 31%
- Substrate costs: 14%
- Phosphor and silicone costs: 10% [7].

Assembly costs are higher for COB LEDs than other LED packages because of the costs associated with placing (e.g., die bonding) and connecting (e.g., wire bonding) the large number of LEDs contained in the device [7]. The cost breakdown for ceramic substrate–based COB LEDs is likely to be slightly different because of the added costs of making the ceramic substrate.

Although the use of COB LEDs in lighting applications is growing, the reliability of this package platform is not as well understood as the MP-LEDs and high-power LEDs (HP-LEDs). A previous study from the U.S. Department of Energy (DOE) used LM-80 data to examine commercial COB LED products. The findings from this study indicated that COB LEDs could be operated in a way that produces high LFM. However, the chromaticity shift behaviors of the COB LEDs were less uniform, and there was no consensus behavior among different manufacturers [8]. It is anticipated that the primary failure mechanisms of COB LEDs will be related to the density of waste heat that is produced and the increased probability of excess moisture penetration through the large silicone LES. Among the heat-related effects that could arise in COB LEDs are changes in the phosphors through quenching and thermal photo-oxidation that impact phosphor emission efficiency, which would appear as a loss of LFM or change in chromaticity. In addition, changes in packaging materials such as Ag corrosion could also impact COB LED performance by reducing the reflectance of the substrate. Consequently, it is important to test COB LED devices at both normal operating conditions and at stressed conditions to understand the factors that are responsible for luminous flux decay and chromaticity shifts in this packaging platform. Given the lack of information about COB LED reliability, the goal of this study was to benchmark COB LED performance in several different environments in preparation for future accelerated stress tests (ASTs) at more severe conditions to study COB LED failure modes.

2 Experimental Methods and Analytics

This study focused on determining the construction of a group of commercially available COB LED products and evaluating their performance in room temperature operating life (RTOL) and 75 degrees Celsius (°C) operational life (75OL) tests. Testing is also being conducted at other conditions, but those studies are still in progress; comprehensive results from different AST protocols will be given in future reports.

2.1 Samples

For convenience, the devices under test (DUTs) examined during this study are referred to by using the designation Product COB-X, in which "X" is a number from 1 to 6, and all DUTs of the same designation were equivalent at the beginning of any testing. Most of the COB LED products have fixed CCT values, although the CCT values for Products COB-1 and COB-3 are tunable. Product COB-1 is a dim-to-warm device that has been discussed previously [4,5], whereas Product COB-3 is a tunable-white device with LED primary emissions at 2,700 K and 6,500 K. Product COB-3 can be tuned to CCT values between the two endpoints by adjusting the current to each LED primary as previously described [9,10]. The LES of the COB LED DUTs were circular with a diameter that ranged from 4.5 millimeters (mm) to 14.6 mm. The color rendering index (CRI) values of all of the COB LED DUTs except for Products COB-4 and COB-5 are greater than 90 (discussed in **Section 3** of this report).

A tunable-white MP-LED product was also included in the test matrix for comparison purposes; this product was designated as Product MS-6, where the abbreviation MS means modified spectrum and refers to the ability of the device to change spectrum by tuning. Product MS-6 is a single LED package mounted onto a star board. Inside the MP-LED package are two separate LED circuits, each containing an LED die that is mounted on an Ag-plated lead frame. One die is tuned to a nominal CCT value of 2,700 K; the other die is tuned to a nominal CCT value of 6,500 K. Product MS-6 contains four electrodes, an anode and cathode for each circuit (i.e., LED die) allowing the two circuits to be operated independently. Consequently, the CCT value of light produced from this package can be varied linearly between 2,700 K and 6,500 K by changing the I_f values supplied to each die. A photograph of Product MS-6 is shown in **Figure 2-1**. Details about the construction and physical properties of the DUTs examined in this study are in **Table 2-1**.

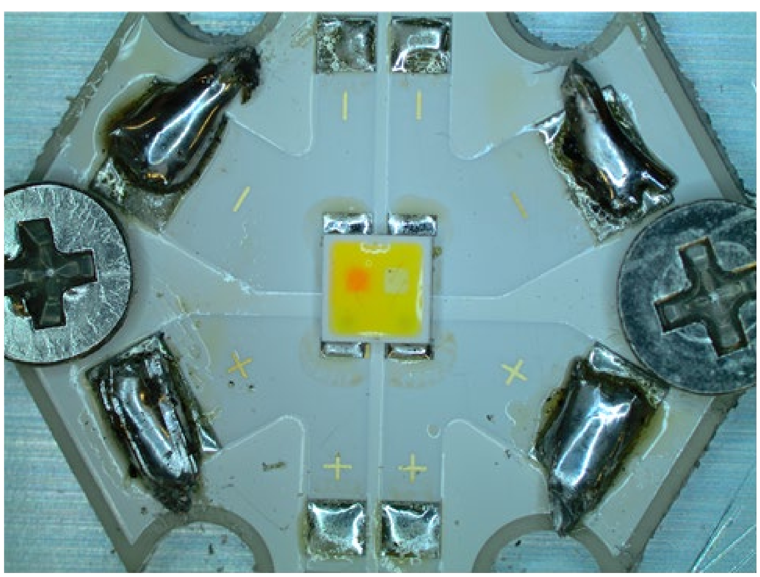

Figure 2-1: The Product MS-6 device was included in this study as a comparison with the COB LEDs.

Table 2-1: Construction and physical characteristics of the DUTs examined during this study.

Product	Package Size (mm)	LES Size (mm)	COB LED Substrate	Nominal CCT (K)
COB-1	15 mm × 12 mm	9.3 mm diameter	MCPCB	Variable (1,800 K–3,000 K)
COB-2	36.2 mm diameter[a]	13 mm diameter	MCPCB	2,700 K
COB-3	18.8 mm × 18.8 mm	14.2 mm diameter	MCPCB	Variable (2,700 K–6,500 K)
COB-4	15.9 mm × 15.9 mm	8.9 mm diameter	Dielectric on ceramic—AlN	2,700 K
COB-5	13.4 mm × 13.4 mm	4.5 mm diameter	MCPCB	2,700 K
COB-6	24 mm × 24 mm	14.6 mm diameter	Ceramic—Al_2O_3	5,000 K
MS-6	3 mm × 3 mm	2.6 mm × 2.6 mm	Heat-resistant polymer	Variable (2,700 K–6,500 K)

[a] The package size for Product COB-2 includes the COB LED holder. The MCPCM size is 16.5 mm × 16.5 mm.

The size of the LED die used in the COB LED and MP-LED package platforms are similar, but the number of die is much higher in a COB LED package than in a MP-LED package. The number of LED die within each COB LED DUT ranged from a high of 108 (Product COB-6) to a low of 12 (Product COB-5). The individual LED die sizes are similar between the DUTs as shown in **Table 2-2**, although there were some variations in die size between the different samples. Because LED size was similar in MP-LEDs and COB LEDs, the use of Product MS-6 for comparison purposes was further justified. However, the operational temperature of Product MS-6 was much lower than any COB product because of the reduced amount of waste heat that was produced in the package with only two LED die.

Table 2-2: Characteristics of the LEDs in each DUT.

Designation	Number of LED Die	LED Die Size (mm)	Die Edge-to-Edge Pitch (mm)	Die Connection	Interconnect Method
COB-1	21	0.8 x 0.7	Smallest: 0.3 Largest: 2.3	4 parallel strings with: 1 string containing 4 LEDs in series 1 string containing 5 LEDs in series 2 strings containing 6 LED series	Wire bond
COB-2	33	1.2 x 0.6	0.8	3 parallel strings of 11 LEDs in series	Wire bond
COB-3	84	0.8 x 0.7	0.4	7 parallel strings of 12 LEDs in series	Wire bond
COB-4	24	1.1 x 1.1	0.3	2 parallel strings of 12 LEDs in series	Flip chip
COB-5	12	0.8 x 0.7	0.2	2 parallel strings of 6 LEDs in series	Wire bond
COB-6	108	0.7 x 0.7	0.5	9 parallel strings of 12 LEDs in series	Wire bond
MS-6	2	0.7 x 0.7	0.4	LEDs in parallel operated separately	Wire bond

A photograph of the COB DUTs as received is shown in **Figure 1-1**; photographs of the DUTs that have been successfully decapped are provided in **Appendix A**.

2.2 Experimental Procedures

2.2.1 Heat Sink Selection

Because COB LEDs contain many individual LED die, the junction temperature (T_j) is not necessarily the same for all die. Therefore, the case temperature (T_c) of the COB LED is typically used for monitoring temperature exposure, and this parameter can be monitored through the electrodes or a designated location on the COB LED package. To provide appropriate thermal management, extruded Al heat sinks of the same finning architecture were purchased from HeatSinks USA and were used for all DUTs in this study. According to the manufacturer, the thermal resistance between the heat sink and ambient air (Θ_{sa}) is 4.5 degrees Celsius per watt (°C/W) for a 7.62 centimeter (cm; i.e., 3 inches)–long segment of heat sink. The thermal resistance of other heat sink lengths can be calculated by using standard correction factors for length and temperature gradient [11]. The physical properties of the heat sinks used in this study are given in **Table 2-3**, along with the number of DUTs mounted on each heat sink. The length of the heat sink for all products was chosen so that the T_c value of the COB LED DUTs stayed at or below the maximum value specified by the COB LED manufacturer. The length of the heat sink was not optimized once these conditions were met. The interface between each DUT and the heat sink was filled with a thin layer (estimated to be 0.01 cm) of silicone-based thermal grease (Halnziye HY410) that serves as a thermal interface material (TIM). The thermal resistance of the TIM is essentially the thermal resistance between the case and the heat sink (Θ_{cs}) and is given as less than 0.704 degrees Celsius meter per watt (°C-m/W) by the manufacturer.

Table 2-3: Properties of the different heat sinks used during this study.[a]

DUT	Number of DUTs per Heat Sink	Number of LEDs per Heat Sink	Heat Sink Dimensions (cm)	Heat Sink Weight (grams [g])
COB-1	3	63	12.7 × 4.6 × 3.1	232
COB-2	1	33	25.4 × 4.6 × 3.1	440
COB-3	1	84	25.4 × 4.6 × 3.1	440
COB-4	1	24	25.4 × 4.6 × 3.1	440
COB-5	2	24	25.4 × 4.6 × 3.1	440
COB-6	1	108	25.4 × 4.6 × 3.1	440
MS-6	1	2	2.5 × 4.6 × 3.1	44

[a] The finning structure on all heat sinks was the same and consisted of six evenly spaced, vertical fins of 2.4-cm length across the 4.6-cm width of the heat sink.

A maximum T_c of 105°C for each DUT was determined based on information in the manufacturers' specification sheets, and appropriate de-ratings were applied to the current levels to stay with this temperature. These experimental parameters are listed in **Table 2-4**. During RTOL tests, the DUTs were operated in still air, and the T_c could be calculated by taking into account the waste heat generated by the LEDs, the thermal resistance of the TIM, and the thermal resistance of the heat sink. During 75OL tests, there was a constant air flow over the DUTs caused by the circulating fan in the environmental chamber. For these samples, T_c was determined by measuring the heat sink temperature and adding in the product of the maximum thermal power being dissipated and the thermal resistance of the TIM. In all calculations, the LEDs were assumed to be 30% efficient, which means that the maximum thermal power being dissipated was $0.7V_fI_f$.

Table 2-4: RTOL and 75OL operational conditions for DUTs reaching at least 6,000 cumulative hours of testing.

Product	Nominal I_f	T_c in RTOL (°C)	T_c in 75OL (°C)	Maximum Allowed T_c (°C)[a]
COB-1	350 mA	72	87	105
COB-2	500 mA	68	85	105
COB-3	500 mA for each active primary	70 (One primary) 113 (Both primaries)	108	105
COB-5	500 mA	77	85	125
MS-6	90 mA for each active primary	28	78	120[b]

[a] Based on the manufacturer's specifications.
[b] This value is the T_j for Product MS-6.

2.2.2 Testing Procedures

The DUTs were mounted on appropriate heat sinks and continuously operated in still air at room temperature or at an elevated ambient temperature of 75°C in an environmental chamber with high air circulation for an extended period. The DUTs in 75OL also sat on metal racks, which helped with heat dissipation. For most DUTs, the operational time was at least 6,000 hours (hrs) of RTOL or 75OL tests in a continually powered state. DUTs that were recently added to the test matrix (i.e., Products COB-4 and COB-6) have experienced fewer test hours at this time; their performance will be provided in future reports.

Photometric measurements were taken for all DUTs before testing and after every 1,000 hrs of RTOL tests by using procedures described in **Section 2.2.4** of this report. After photometric testing, the DUTs were returned to RTOL or 75OL exposure for continued testing.

2.2.3 LED Decapping Methods

The decapping operation consisted of immersing the DUTs in a series of solutions. First, the devices were immersed in deionized water for 5 seconds (sec), and then in a degreasing solution (eOx Economic Cleaner and Degrease) for 5 sec, followed by another 5-sec rinse in deionized water. Then, the LED module was immersed in the decapping agent (PolyGone 505). The DUTs with small LESs could be decapped within 20 to 30 minutes (min) of immersion, but the larger LES DUTs required overnight immersion. DUTs set to a single CCT value were typically easier to decap than tunable DUTs, which often contained silicone of different durometers slowing the decapping process. In some cases, the DUTs were ultrasonicated for 10 to 20 min toward the end of the decapping process, although ultrasonication time was tightly controlled to minimize damage to the DUTs (e.g., wire bond breakage) and satisfactory decapping was not achieved. For Product COB-1, hours of soaking in the decapping solution were not sufficient to remove all of the phosphors. For Product COB-5, this short decapping time also caused dissolution of the thermal conductor between the LED die and the metal substrate, which affected operation of the decapped products. The best decapping results were obtained with Product COB-4, and acceptable results were achieved with Products COB-2, COB-3, and COB-6. Product MS-6 was also relatively easy to decap when using this procedure. Photographs of the decapped products are available in **Appendix A**. After removal of the phosphor-silicone mixture, the DUT was rinsed with water for 5 sec, dunked into the degreasing solution for 5 sec, and rinsed again in water for 5 sec. Phosphor particles in the decapping solution were collected by using filter paper (StonyLab 50 mm) and a Buchner funnel. The filter paper and collected material were dried and stored for layer analysis.

Upon completion of the process, each LED module was inspected with an Olympus SZ61 stereomicroscope (zoom range 0.67x to 4.5x) to ensure that the silicone and phosphors had been removed. The microscope is equipped with an Olympus SC30 camera that allowed photography of the decapped LEDs to study the structure inside the package.

2.2.4 Photometric Measurement Methods

The spectral power distribution (SPD), luminous flux, radiant flux, and chromaticity of all samples were measured at room temperature in either a calibrated 65-inch integrating sphere or a calibrated 10-inch integrating sphere. The 65-inch sphere was used to measure all COB LED DUTs, whereas the 10-inch integrating sphere was used to measure only Product MS-6. For all integrating sphere testing, the DUTs were mounted in the center of the sphere (4π geometry). Regular calibrations of the integrating sphere were performed by using a calibrated spectral flux standard that was traceable to standards from the National Institute of Standards and Technology (NIST). Background corrections were applied prior to calibration. Self-absorption corrections were made for all samples by using an auxiliary lamp mounted inside the sphere; this process is in accordance with procedures in the joint American National Standards Institute (ANSI) and Illuminating Engineering Society (IES) standard ANSI/IES LM-79-19 [12]. The center post was used to supply direct current (dc) to all DUTs. For the COB LEDs, dc power was provided by a driver preset to the appropriate I_f value. For Product MS-6, dc was provided by two source meters (Keithley 2400), one for each circuit.

3 Results

3.1 Initial Photometric Benchmarks of White LEDs

Initial photometric benchmarks were acquired on all DUTs included in this study. The SPDs of all products were measured, and the results are given in **Appendix B**. Several photometric measures were calculated from the SPDs, including the nominal CCT, the LED maximum emission wavelength ($\lambda_{LED,max}$), and the phosphor maximum emission wavelength ($\lambda_{phos,max}$). In addition, the color fidelity (R_f) and color gamut (R_g), metrics were calculated by using the ANSI/IES TM-30-18 calculator [13]. These metrics are summarized in **Table 3-1** for each DUT, and the full reports from the basic TM-30-18 calculator are given in **Appendix C**. **Table 3-1** also includes the general colors of the secondary emissions from the phosphors used in the DUTs; the general colors are intended to be a guide.

Table 3-1: Initial photometric characteristics of the DUTs examined during this study.

Product	Nominal CCT (K)	R_f, R_g	$\lambda_{LED,max}$ (nm)	Phosphor Emission Colors	$\lambda_{phos,max}$ (nm)
COB-1 (warm dimmed)	1,800	93, 99	453	Green, red	646
COB-1 (warm)	3,000	95, 102	454	Green, red	634
COB-2	2,700	91, 98	453	Green, red	621
COB-3 (warm)	2,700	93, 97	454	Green, red	622
COB-3 (neutral)	4,300	92,100	454	Green, red	622
COB-3 (cool)	6,800	89, 97	454	Green, red	553
COB-4	2,700	85, 98	446	Green, red	609
COB-5	2,700	86, 98	450	Green, red	606
COB-6	5,000	98, 101	422	Blue, green, red	461
MS-6 (warm)	2,600	87, 96	454	Green, red	608
MS-6 (neutral)	3,900	86, 98	453	Green, red	601
MS-6 (cool)	6,200	82, 94	453	Green, red	560

Note: nm = nanometer.

The initial performance of these DUTs can be compared from the standpoint of radiant efficiency (**Figure 3-1**) and luminous efficacy (**Figure 3-2**). For this work, "radiant efficiency" is defined as the ratio of the emitted optical power (in watts) divided by the electrical power injected into the LED (in watts) [14]. The radiant efficiency metric reported here does not include any losses associated with the driver because this value will depend on the driver choice and not the performance of the LEDs. The radiant efficiency of the COB LED DUTs varies from 0.31 (Product COB-5) to 0.44 (Product COB-3 cool white setting). The lowest radiant flux value (Product COB-5) was also the DUT with the smallest LES and the smallest chip-to-chip spacing (see **Table 2-2**). The radiant efficiency of the COB LED DUTs generally increased with CCT value, as shown best by Product COB-3, because of the added losses (e.g., Stokes shift) that occur with warm white phosphors. In contrast, the radiant efficiency of the tunable-white MP-LED package (i.e., Product MS-6) was higher than any of the COB LED DUTs and varied between 0.47 and 0.53. The radiant efficiency of Product MS-6 also increased with CCT value.

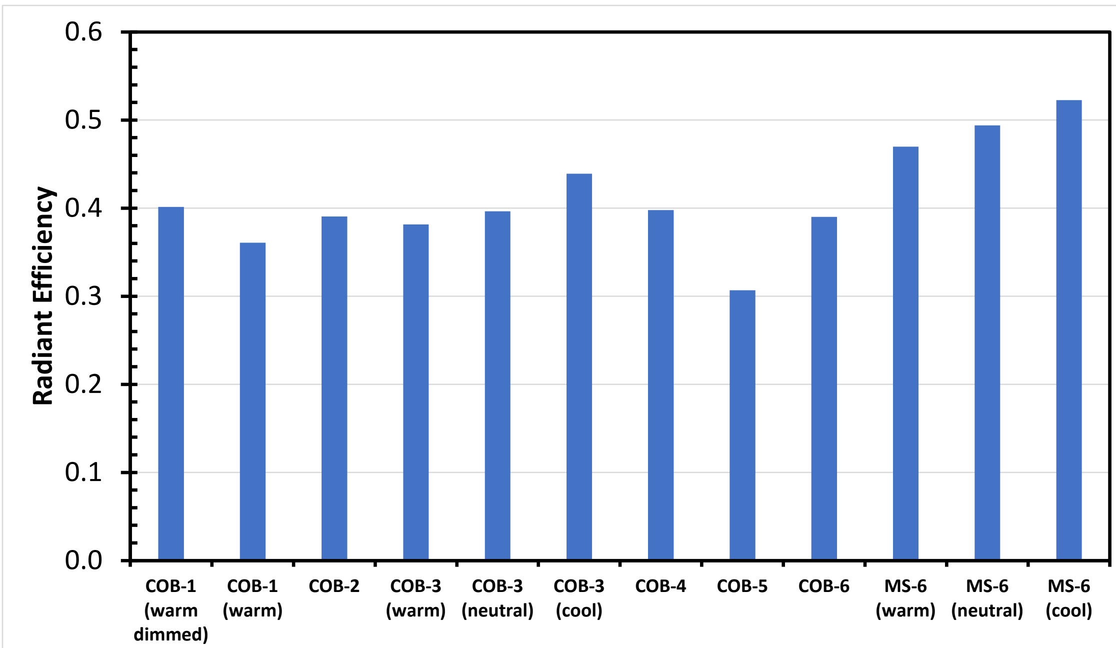

Figure 3-1: Initial radiant efficiency values of the DUTs examined during this study.

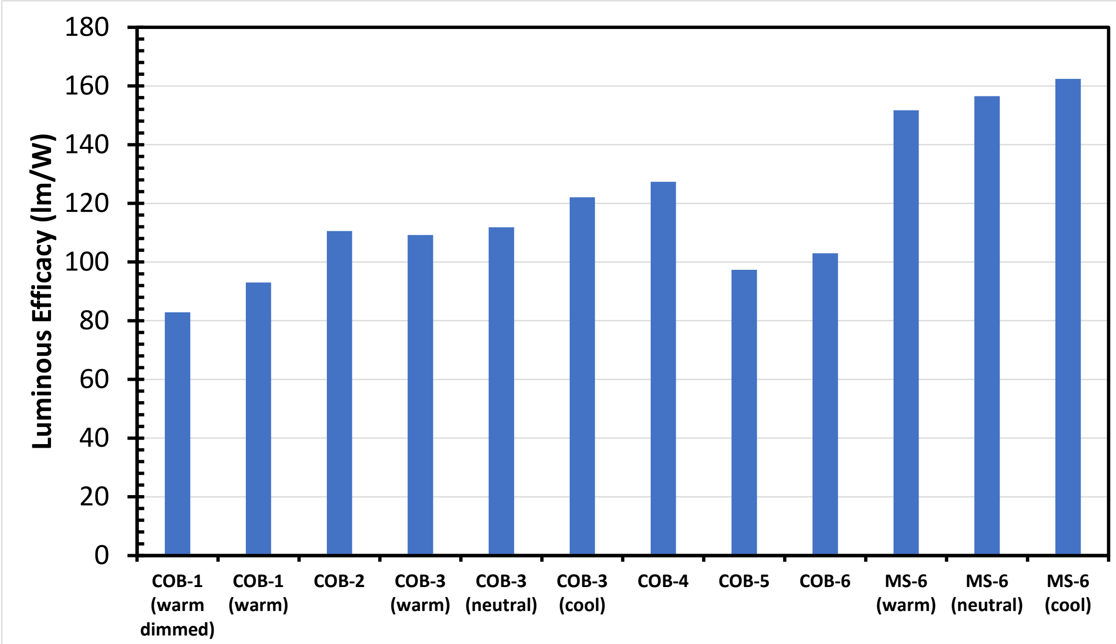

Figure 3-2: Initial luminous efficacy of the DUTs examined during this study.

The "luminous efficacy" of the different DUTs is defined as the ratio of the total emitted luminous flux (in lumens [lm]) and the total source electrical input power (in watts) [14]. In the calculations reported here, only the electrical input power provided directly to the LEDs is included, and any electrical losses associated with the driver are ignored. The luminous efficacies of the COB LED DUTs varied from a low of 83 lm/W (Product COB-1 dim state) to a high of 127 lm/W (Product COB-4). The luminous efficacy of the COB LED DUTs may have some dependence on CCT value (see Product COB-3), although other factors (e.g., interconnect method, thermal management) are also important.

The luminous efficacy of Product MS-6 was significantly higher and varied between 152 and 162 lm/W, depending on the CCT value. This value represents an increase of 20% in the luminous efficacy for Product MS-6 at the warm white CCT compared with Product COB-4. It should be noted that Products COB-4 and Product MS-6 have similar R_f metrics (see **Table 3-1**), and this difference in luminous efficacy rises to 56% when comparing Product MS-6 with Product COB-5, even though they also have similar R_f metrics. Because the LES area of Product MS-6 is only 43% of that of Product COB-5, there are clearly other factors in play that impact luminous efficacy of COB LEDs. The higher luminous efficacy of Product MS-6 may be because of the smaller number of absorbing materials (e.g., LED chips, wire bonds) in the optical path of the devices compared with the COB LED DUTs, the larger die spacing found in Product MS-6, and the lower amount of heat dissipation needed for the two LED die in the MP-LED package compared with the higher die counts in the COB LEDs.

3.2 RTOL Performance

Different populations of the DUTs examined during this study are undergoing different ASTs. In this section of the report, the RTOL testing results are presented for the DUTs that have reached a minimum of 6,000 hrs of testing. Similar measurements were taken for separate populations in 75OL and are given in **Section 3.3**. The operational conditions for DUTs discussed in this study are shown in **Table 2-4**. RTOL data were previously reported for Product COB-1 (see results for Module E in earlier reports [5,6]). This report extends the RTOL data for Product COB-1 to 16,000 hrs and provides an updated LFM model. LFM behavior in RTOL is also reported here for Products COB-2 and COB-3, both of which have reached the required 6,000 hrs of testing. Some data for Product COB-5 are included because it has reached 5,000 hrs of testing and a chromaticity trend has emerged during RTOL but not an LFM trend. Data for Products COB-4 and COB-6 are not included here because these DUTs have not reached 6,000 hrs of RTOL testing; these data will be presented in a future report.

3.2.1 RTOL LFM

During RTOL tests, the LFM behavior of the DUTs was generally excellent, with LFM values of at least 0.93 for the test duration of each DUT. These LFM values are reported in **Table 3-2**. Some data for Product COB-5 are included in **Table 3-2**, but TM-21-19 models were not calculated because the DUTs have not reached the requisite 6,000 hrs of testing.

Table 3-2: LFM and ANSI/IES TM-21-19 model parameters for the DUTs examined during this study.

Product	Nominal CCT (K)	Test Duration (hrs)	LFM at Test Termination	α Value	B Value
COB-1 (warm)	3,000	16,000	0.94	2.6×10^{-6}	0.98
COB-2	2,700	6,000	1.00	2.0×10^{-6}	0.99
COB-3 (warm)	2,700	6,000	1.00	2.0×10^{-6}	0.97
COB-3 (neutral)	4,300	6,000	0.99	2.0×10^{-6}	0.96
COB-3 (cool)	6,800	6,000	1.00	2.0×10^{-6}	0.97
COB-5	2,700	5,000	0.96	[a]	[a]
MS-6 (warm)	2,600	11,000	0.93	2.0×10^{-6}	0.94
MS-6 (neutral)	3,900	11,000	0.95	2.0×10^{-6}	0.96
MS-6 (cool)	6,200	11,000	0.95	3.3×10^{-6}	0.99

[a] Testing has not reached the 6,000-hr minimum duration required in ANSI/IES TM-21-19; therefore, α and B cannot be calculated at this time.

ANSI/IES TM-21-19 is the established method for modeling and projecting the long-term LFM of LED sources, including LED packages and arrays, and is used here to model the behavior of the COB LEDs [15]. ANSI/IES TM-21-19 uses a single-exponential model to describe the change in the luminous flux at any time ($\Phi(t)$) compared with the initial luminous flux (Φ_0), and the model can be expressed as shown in **Equation 3-1** as follows:

$$\Phi(t) / \Phi_0 = Be^{-\alpha t} \qquad \text{(Eq. 3-1)}$$

where
B = Projected initial constant derived from least squares curve-fit
α = Decay rate constant
t = time.

One of the restrictions of ANSI/IES TM-21-19 is that the decay rate constant (α) cannot be less than 2.0×10^{-6} [15]. Computed values of α below that threshold must be given the value of 2.0×10^{-6}. As shown in **Table 3-2**, most of the DUTs in the 75OL tests were given α values of 2.0×10^{-6}, in keeping with the excellent LFM performance observed for these DUTs.

3.2.2 RTOL Chromaticity Maintenance

There are two elements of chromaticity shift that also need to be examined for these DUTs: the magnitude of the chromaticity shift reported as $\Delta u'v'$ and the direction of the chromaticity shift. The magnitude of the chromaticity shift ($\Delta u'v'$) is given by **Equation 3-2** as follows:

$$\Delta u'v' = \sqrt{[(u'(t) - u_0')^2 + (v'(t) - v_0')^2]} = \sqrt{[(\Delta u')^2 + (\Delta v')^2]} \qquad \text{(Eq. 3-2)}$$

where
$u'(t)$ = The u' chromaticity coordinate measured at time, t
u'_0 = The initial value of the u' chromaticity coordinate
$v'(t)$ = The v' chromaticity coordinate measured at time, t
v'_0 = The initial value of the v' chromaticity coordinate.

The direction of chromaticity shift can be summarized by one of five likely chromaticity shift modes (CSMs) [16,17,18]. The chromaticity shift magnitude values are reported in **Table 3-3** for testing results of Products COB-1, COB-2, COB-3, and COB-5 during RTOL. Products COB-1, COB-2, and COB-3 have completed at least 6,000 hrs of testing. Product COB-5 is included here because a clear chromaticity shift trend has emerged during 5,000 hrs of testing. Graphs of $\Delta v'$ versus $\Delta u'$ are given in **Appendix D**.

Table 3-3: Chromaticity shift magnitude ($\Delta u'v'$) and CSM behavior observed for RTOL tests of the DUTs examined during this study.

Product	Nominal CCT (K)	Test Duration (hrs)	$\Delta u'v'$	CSM
COB-1 (warm)	3,000	16,000	0.0035	CSM-1 + CSM-2
COB-2	2,700	6,000	0.0017	CSM-2
COB-3 (warm)	2,700	6,000	0.0011	Not determined
COB-3 (neutral)	4,300	6,000	0.0010	Not determined
COB-3 (cool)	6,800	6,000	0.0010	Not determined
COB-5	2,700	5,000	0.0035	CSM-2
MS-6 (warm)	2,600	11,000	0.0014	CSM-1 + CSM-2
MS-6 (neutral)	3,900	11,000	0.0021	CSM-1 + CSM-2
MS-6 (cool)	6,200	11,000	0.0013	CSM-1

A variety of factors can cause chromaticity shifts in LEDs and solid-state lighting (SSL) luminaires. Some of these factors include changes in the direct emitter, changes in the phosphors, changes in the optical system (e.g., lenses, reflectors), and, in some cases, changes in the electrical system [16,17,18]. These chromaticity changes generally produce a larger shift in one chromaticity coordinate (i.e., u', v') than the other, although there are instances where significant shifts occur simultaneously along the u' and v' axes, suggesting that two CSMs may be active. The CSM can be identified by the change in the u' and v' chromaticity coordinates from the original (i.e., $t = 0$) value, which is denoted as $\Delta u'$ and $\Delta v'$. The chromaticity coordinate change (i.e., $\Delta u'$, $\Delta v'$) is positive when the chromaticity coordinate (i.e., $u'(t)$, $v'(t)$) measured at time, t, is larger than the initial value and is negative when the initial chromaticity coordinate is larger than the value measured at time, t. The principal CSMs are as follows:

- CSM-1—A shift mainly in the $-\Delta v'$ chromaticity coordinate toward the generally blue direction
- CSM-2—A shift mainly in the $-\Delta u'$ chromaticity coordinate toward the generally green direction
- CSM-3—A shift mainly in the $+\Delta v'$ chromaticity coordinate toward the generally yellow direction
- CSM-4—A complex shift that has an interim shift in the $+\Delta v'$ chromaticity coordinate toward the generally yellow direction, followed by a final shift in the $-\Delta v'$ chromaticity coordinate toward the generally blue direction

- CSM-5—A shift mainly in the + $\Delta u'$ chromaticity coordinate toward the generally red direction.

The direction of chromaticity shift corresponding to each CSM is shown on the 1976 International Commission on Illumination (*Commission Internationale de l'Éclairage* [CIE]) uniform color space in **Figure 3-3**.

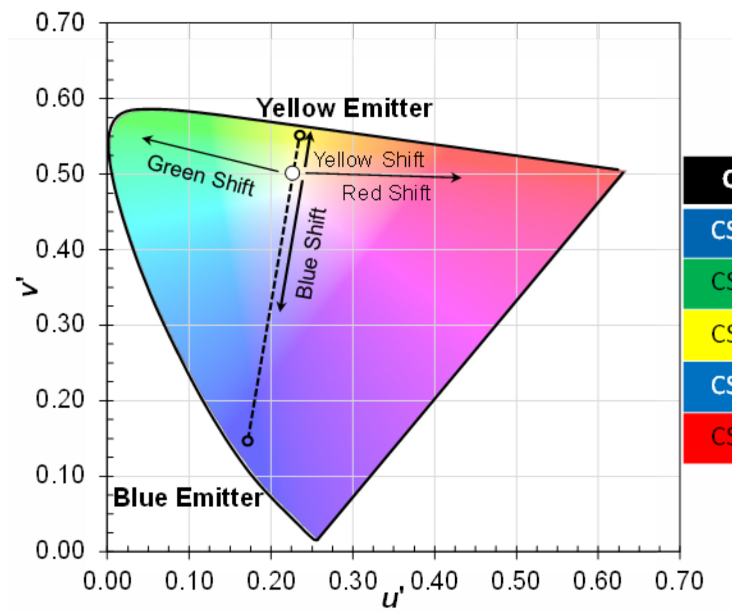

CSM	Terminal Shift Direction
CSM-1	Blue
CSM-2	Green
CSM-3	Yellow
CSM-4	Yellow then Blue
CSM-5	Red

Figure 3-3: Chromaticity shift directions for LED devices in the CIE 1976 color space. The initial chromaticity point is the white circle, and the chromaticity points of the blue and yellow emitters are also shown

The DUT population with the most rapid chromaticity shift during the RTOL tests was Product COB-5, which exhibited a $\Delta u'v'$ value of 0.0035 after 5,000 hrs of testing. Most of the chromaticity change for Product COB-5 was along the -$\Delta u'$ axis, indicating CSM-2 behavior. The next largest chromaticity shift was observed for Product COB-1 after 16,000 hrs of testing. Product COB-1 exhibited a steady change along the -$\Delta u'$ direction, indicating CSM-2 behavior. There was also a sharp change in chromaticity along the -$\Delta v'$ axis during the first 3,000 hrs of testing, indicating that CSM-1 behavior was also occurring. Products COB-2 and COB-3 exhibited minimal chromaticity shift ($\Delta u'v' \leq 0.002$) after 6,000 hrs of RTOL operation, and the direction of their chromaticity shifts could not be determined. Products COB-4 and COB-6 have not been operated long enough to establish a reliable determination of chromaticity shift behavior.

3.3 75OL Performance

3.3.1 75OL LFM

The LFM of the COB LED and Product MS-6 DUTs examined in 75OL are shown in **Figure 3-4** and **Figure 3-5**, respectively. The data are only presented for Products COB-2, COB-3, and COB-5 because these DUTs have completed at least 6,000 hrs of testing in 75OL. The LFM behavior of Product COB-1 was previously provided after 7,000 hrs of testing in an operational life test at 45°C (45OL) and will not be repeated here [5,6]. Products COB-4 and COB-6 have not completed 6,000 hrs of testing during 75OL; therefore, their behavior will be reported later.

The data from the tested COB LED DUTs were fitted with an exponential decay model according to ANSI/IES TM-21-19 [15], and the results of these fit parameters are presented in **Table 3-4**. The LFM of the COB LED

DUTs in 75OL was greater than 0.95 for the first 3,000 hrs of 75OL exposure. Then, the LFM began to decline rapidly between 3,000 and 6,000 hrs, and this decay rate was much faster for Product COB-3 than for Products COB-2 and COB-5 (see **Figure 3-4**). This finding suggests a change in LFM mechanism beginning at approximately 3,000 hrs of 75OL operation. In contrast, the LFM values of Product MS-6 DUTs remained above 0.91 through 11,000 hrs of 75OL exposure (see **Figure 3-5**). The difference between the LFM behavior for the COB LED DUTs and Product MS-6 DUTs is likely the consequence of the higher operational power levels and higher T_c values of the COB LEDs relative to Product MS-6. In addition, the increase rate of luminous flex loss for Product COB-3 between 3,000 and 6,000 hrs may be a consequence of slightly exceeding the recommended T_c and I_f values in these tests (see **Table 2-4**). However, both the T_c and I_f values also exceed the manufacturer's specification during the RTOL tests and there was no significant impact on LFM. Therefore, the reason for the higher α values during the 75OL tests compared with the RTOL tests is unknown. It is worth noting that the environmental chamber containing the Products COB-2 and COB-3 DUTs experienced a one-time and unexpected temperature excursion near the 4,000-hr test duration mark that lasted for 24 hrs. However, the Product COB-2 DUTs also experienced this heat excursion and were less affected.

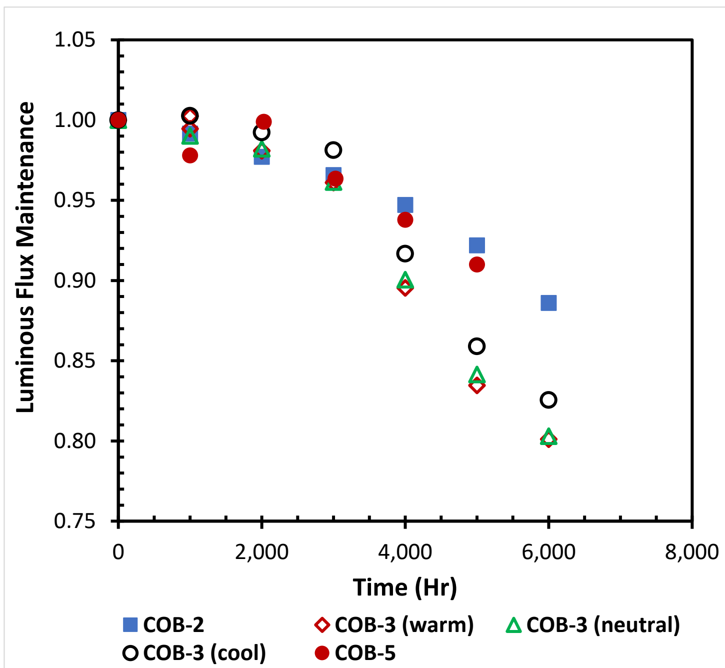

Figure 3-4: LFM for the COB LED DUTs examined during the 75OL tests.

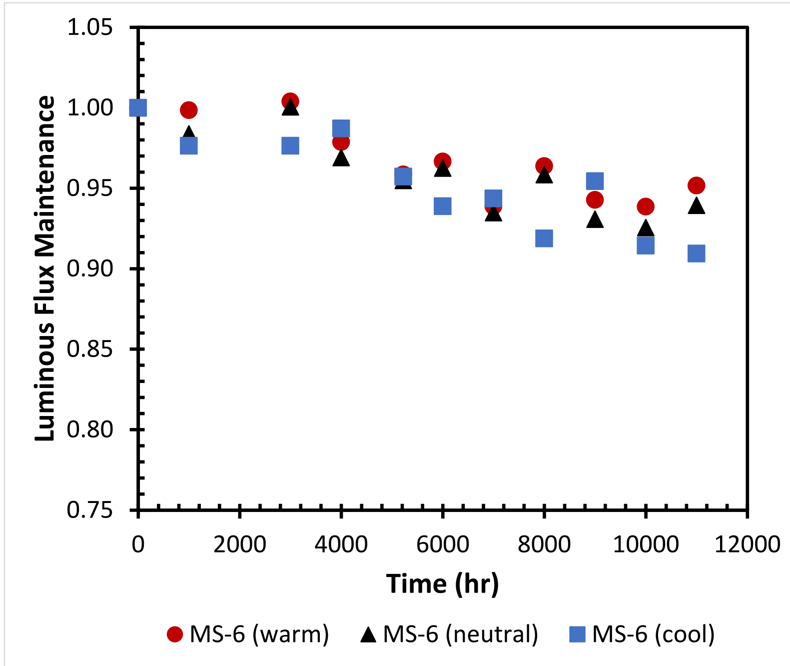

Figure 3-5: LFM for the Product MS-6 DUTs examined during the 75OL tests.

Table 3-4: ANSI/IES TM-21-19 parameter models for DUTs examined during the 75OL tests.

Product	Nominal CCT (K)	Test Duration (hrs)	LFM at Test Termination	*α* Value	*B* Value
COB-2	2,700	6,000	0.89	2.2×10^{-5}	1.02
COB-3 (warm)	2,700	6,000	0.80	4.5×10^{-5}	1.06
COB-3 (neutral)	4,300	6,000	0.80	4.5×10^{-5}	1.07
COB-3 (cool)	6,800	6,000	1.00	4.2×10^{-5}	1.07
COB-5	2,700	5,000	0.91	[a]	[a]
MS-6 (warm)	2,600	11,000	0.95	2.8×10^{-6}	0.97
MS-6 (neutral)	3,900	11,000	0.94	4.8×10^{-6}	0.98
MS-6 (cool)	6,200	11,000	0.91	7.1×10^{-6}	0.99

[a] Testing has not reached the 6,000-hr minimum duration required in ANSI/IES TM-21-19; therefore, *α* and *B* cannot be calculated at this time.

3.3.2 75OL Chromaticity Maintenance

The chromaticity shift and chromaticity maintenance behavior were recorded after 75OL exposure for Products COB-2, COB-3, and COB-5. Product COB-5 is included here because a clear chromaticity shift trend has emerged through 5,000 hrs of testing. This information was previously reported for Product COB-1 after 45OL exposure and will not be repeated here (see Module E in earlier reports [5,6]). Products COB-4 and COB-6 have not reached the requisite test duration (i.e., 6,000 hrs); therefore, their chromaticity maintenance behavior during the 75OL tests will be provided in a future report. In general, the rate of chromaticity shift recorded for the COB LED DUTs was higher during the 75OL tests than during the RTOL tests, but the same general trends for chromaticity shift direction were observed for both test conditions. A summary of the chromaticity maintenance behavior is provided in **Table 3-5**, and the chromaticity shift diagrams plotting the change in the *v'* component against the change in the *u'* chromaticity coordinate (i.e., *Δv'* versus *Δu'*) are given in **Appendix D**.

Table 3-5: Chromaticity shift magnitude (*Δu'v'*) and CSM behavior observed for 75OL tests of the DUTs examined during this study.

Product	Nominal CCT (K)	Test Duration (hrs)	*Δu'v'*	CSM
COB-2	2,700	6,000	0.0058	CSM-1 + CSM-2
COB-3 (warm)	2,700	6,000	0.0039	CSM-2 then CSM-1
COB-3 (neutral)	4,300	6,000	0.0088	CSM-2 then CSM-1
COB-3 (cool)	6,800	6,000	0.0107	CSM-1
COB-5	2,700	5,000	0.0043	CSM-2 then CSM-1 + CSM-2
MS-6 (warm)	2,600	11,000	0.0015	CSM-2
MS-6 (neutral)	3,900	11,000	0.0021	CSM-1
MS-6 (cool)	6,200	11,000	0.0028	CSM-1

For Product COB-2 DUTs operated in 75OL, the chromaticity shift occurred almost equally along both the *-Δu'* and *-Δv'* axes at each measurement interval as shown in **Figure D-1**. The shift during the RTOL test is in a similar direction, but significantly slower. This behavior suggests that CSM-1 and CSM-2 behaviors are occurring simultaneously.

For Product COB-3, the situation is more complicated. The chromaticity shift for the Product COB-3 (cool) DUTs is mainly along the *-Δv'* axis as shown in **Figure D-4**, and the rate of this shift accelerated after 3,000 hrs of exposure. Ultimately, the chromaticity shift for the Product COB-3 (cool) DUTs reached a magnitude of *Δu'v'* = 0.0107, which can be considered a parametric failure for chromaticity shift. This finding indicates that the CSM-1 shift is the terminal (i.e., emergent) shift for this product in the 6,500 K setting. By comparison, **Figure D-2** demonstrates that the initial shift for the COB (warm) LED DUTs was along the *-Δu'* axis (i.e., CSM-2 behavior), and then the chromaticity started to change along the *-Δv'* axis (i.e., CSM-1 behavior) while also changing along the *-Δu'* axis after 3,000 hrs of testing. These changes in chromaticity shift direction coincide with an increase in the rate of luminous flux depreciation as shown in **Figure 3-4**. For the Product COB-3 (neutral) DUTs, the initial chromaticity shift was mainly along the *-Δu'* axis (i.e., CSM-2 behavior) for the first 3,000 hrs of testing, and then the shift was strongly along the *-Δv'* axis (i.e., CSM-1 behavior) with minimal change along the *-Δu'* axis as shown in **Figure D-3**. The shift in the blue direction occurs after 3,000 hrs, similar to the behavior found in Product COB-3 (cool), and the strong blue shift can also be classified as a terminal (i.e., emergent) shift because it led to parametric failure (*Δu'v'* = 0.0088 after 6,000 hrs of testing). Therefore, the cool white primary is the dominant contributor to this chromaticity shift in both the cool white and neutral white settings. Although the DUTs were in a high stress state during the 75OL tests (as evidenced by the increase in α values), the level of stress likely did not change the failure mechanism—only accelerated it. For Product COB-3, the chromaticity shifts observed during the RTOL and 75OL tests were in the same general direction, but the magnitudes of the shifts were higher during the 75OL tests. This finding suggests that the DUTs were not over-stressed during the 75OL tests, even though the test conditions did exceed the manufacturers specifications. If the DUTs were over-stressed, then we would expect to see new failure modes. Instead, the chromaticity shifts occurred in the same general direction, indicating that the same mechanisms responsible for the chromaticity shift are operating in both conditions.

For Product COB-5, the chromaticity shift direction was mainly along the *-Δu'* axis, although there was also a smaller change along the *-Δv'* axis starting after 3,000 hrs of testing, as shown in **Figure D-5**. This behavior suggests that the CSM-2 mechanism was dominant for most of the 5,000-hr test duration, but there was also a small amount of CSM-1 behavior occurring.

By comparison, the chromaticity shift magnitude of the Product MS-6 DUTs was generally smaller but followed the same general trend as Product COB-3. The chromaticity change for Product MS-6 (cool) DUTs displayed strong CSM-1 behavior as shown in **Figure D-8**, where the change in chromaticity was along the -$\Delta v'$ axis. In contrast, the chromaticity change for Product MS-6 (warm) DUTs was primarily along the -$\Delta u'$ axis, indicating CSM-2 behavior (see **Figure D-6**), while the chromaticity shift for Product MS-6 (neutral) DUTs was between the two (see **Figure D-7**). The smaller chromaticity shift magnitude for the Product MS-6 DUTs compared with the COB LED DUTs was likely the result of the lower waste heat generated in a single MP-LED package.

3.4 Decapped LED Performance

The external quantum efficiency (EQE) of an LED ($\eta_{LED,EQE}$) describes the efficiency of light emission from the LED into the surrounding medium. The $\eta_{LED,EQE}$ is defined as the number of photons emitted externally divided by the number of carriers passing the junction (i.e., the number of injected electrons) as shown in (**Equation 3-3** [19] as follows:

$$\eta_{LED,EQE} = \frac{\text{number of photons emitted externally}}{\text{number of carriers passing junction}} = \frac{\Phi_e/hv}{I/e} \qquad \text{(Eq. 3-3)}$$

where

Φ_e = Radiant flux

hv = Photon energy at the emission frequency, v (h is Planck's constant)

I = Injection current

e = Electron charge.

The number of photons emitted externally from the LED (Φ_e/hv) is the product of the efficiency of converting carrier electrons to photons within the LED and the extraction efficiency of the photons from the package. The efficiency of converting carrier electrons to light depends on the properties of the epitaxial layer in the LED. The extraction efficiency, however, depends on the structure of the LED (e.g., surface roughness, shape) and the index of refraction of the surrounding medium, with better extraction efficiency expected when the LEDs are covered in silicone material than when radiating directly to air. This is because of a better match of index of refraction between LEDs (e.g., gallium nitride [GaN] of approximately 2.4) and silicones (1.45 to 1.55) as compared with air (1.0).

With DUTs such as COB LEDs, there are many die and interconnects within the LES, and these surfaces are potential points of light absorption. Furthermore, the reflectivity of the substrate surface (i.e., metal versus ceramic) plays a role in the extraction efficiency. The extent of these differences will vary by package size and type. The LES size, COB LED substrate, LED die size, and number of LED die for the DUTs in this study are presented in and . The LES size (4.5 mm to 14.6 mm) and number of LED die (12 to 108) varied widely between COB LED samples, but the COB LED substrate and LED die size were similar except for Product COB-4, which was flip-chip bonded. Most of the DUTs (except Products COB-4 and COB-6) used an MCPCB, and although the reflectance of the metal substrates was not measured, they are assumed to be similar. The area of a single LED die was similar for most DUTs (0.0049 square centimeters [cm^2] to 0.0072 cm^2) except for Product COB-4 (0.0121 cm^2) and all DUTs except those of Product COB-4 used Au wire bonds for electrical connections.

The $\eta_{LED,EQE}$ values determined from this analysis are presented in **Table 4-1**. The values typically fell into the range of 0.50 and 0.67 when operated at a current density of approximately 18 milliamperes per square centimeter (mA/cm^2). A uniform current density was used in the EQE evaluation to allow a comparison between the different DUTs. The standard test conditions provided in **Table 2-4** do not account for similar current densities between the DUTs.

Table 4-1: EQE of the LEDs at similar current density.

Product	Estimated $\eta_{LED,EQE}$	I_f (mA, LED Chip)	Current Density (A/cm^2)	Surface Area of LED Die to LES (%)
COB-2	0.54	136	18.84	17.9
COB-3 (6,500 K LED primary)[a]	0.50	100	17.86	47.0
COB-4	0.67	218	17.98	46.7
COB-6[b]	0.46	57	11.68	31.6
MS-6 (2,700 K LED primary)	0.66	90	18.41	14.5
MS-6 (6,500 K LED primary)	0.66	90	18.32	14.5

[a] The 2,700 K LED primary failed before it could be characterized. It is expected that the $\eta_{LED,EQE}$ for the 2,700 K LED primary would be the same as the 6,500 K LED primary.

[b] It was not possible to measure Product COB-6 at higher current densities during this testing because of slight dissolution of the thermally conductive material used to bond the LED die to the ceramic substrate (at high current densities, heat dissipation was not sufficient and the LEDs failed).

Overall, even though COB-X products have higher ratios of surface area of the LED die with respect to the LES, good $\eta_{LED,EQE}$ can be achieved. In the data set studied here, Product COB-4 had the highest $\eta_{LED,EQE}$ (0.67), whereas Product COB-6 had the lowest (0.46). The higher value observed for Product COB-4 could be because of any number of factors, including a more efficient epitaxial layer in the blue LEDs, higher reflection of the AlN substrate, and better extraction of the flip-chip LEDs or any combination thereof. The lower value for Product COB-6 likely reflected the lower efficiency of violet LEDs relative to blue LEDs.

The $\eta_{LED,EQE}$ of Products COB-1 and COB-5 could not be determined by using the decapping methods in this current study. Product COB-1 used more than one silicone material, and the durometer and solubility of these materials were very different; with the current method, it was not possible to remove the center silicone without damaging the LEDs along the sides of the COB package. The die bond adhesive for Product COB-5 was soluble in the silicone decapping solution, and that caused the LED die of Product COB-5 to disconnect from the MCPCB. Because of the absence of good thermal contact, an appropriate spectrum could not be obtained from the decapped products. If an appropriate method is found to decap Products COB-1 and COB-5, then EQE values for these products will be included in a future report.

4 Discussions

COB LEDs are an advanced packaging platform for LEDs that offer the benefits of high light intensity in a small and thin package that typically has only two electrical leads. The high light intensity of the COB LED package platform is derived from the large number of LED die contained within its LES. However, the large number of interconnected LED die in a relatively dense COB LED package also produce large amounts of waste heat in a small area that must be handled by the package substrate, which is typically either an MCPCB or a ceramic substrate. Although the MP-LED and HP-LED package platforms have been in use for more than a decade, the COB LED packaging platform is a relatively new LED package for the lighting industry (however, COB packages have been available for other electronic devices for several decades [20]). The COB LED packaging platform shares some similarities with both the MP-LED and HP-LED packaging platforms. The sizes of the LEDs used in the COB LED packaging platform are similar to those used in MP-LEDs, and the thermal management issues of the COB LED packaging platform are somewhat analogous to but usually larger than that of HP-LEDs. However, the production volumes of COB LEDs do not currently equal that of either MP-LEDs or HP-LEDs; therefore, there is less experience with this LED package platform and less is known about its reliability.

Recently, a study of the performance of the four major LED package platforms was conducted by analyzing commercial LM-80 data from products made between 2015 and 2019 [8]. This study included data from 31 COB LED products from Tier 1 LED manufacturers, and the test conditions included T_c values ranging between 55°C and 105°C and I_f values between 375 mA and 3,300 mA. In general, the LFM performance was found to be excellent with the largest α values being 5.4×10^{-6} from a 14-mm LES operated at an I_f value of 900 mA (45 V) and a T_c value of 85°C. This study also examined the chromaticity shift behavior of the COB LED products in the analysis. All products contained in this analysis were warm white COB LEDs with CCT values ranging between 2,682 K and 3,255 K. Unfortunately, only one-third of the COB LED products in this analysis contained chromaticity coordinates, which allowed the $\Delta u'v'$ values and the CSMs to be determined. For these products, a maximum value of $\Delta u'v' = 0.0052$ was calculated based on 15,000 hrs of experimental data. In addition, the following three distinct chromaticity shift behaviors were observed for the COB LED products during the LM-80 study:

- A continuous shift in the generally blue direction, indicative of CSM-1 behavior
- A large initial shift in the generally green direction, indicative of CSM-2 behavior, followed by little to no future shift
- A shift between these two extremes, consisting of an initial shift in the green direction followed by a continuous shift in the blue direction, suggesting that both CSM-1 and CSM-2 behavior were occurring.

In the current study, the luminous flux and chromaticity maintenance of various COB LEDs were examined during the RTOL and 75OL tests. The COB LEDs were mounted on appropriate heat sinks as described in **Section 2.2.1**. The RTOL tests were conducted in a room temperature environment without any forced air flowing over the heat sink. As a result, the T_c values of the COB LEDs during RTOL tests ranged from 68°C to 113°C as shown in **Table 2-4**. The exposure of the COB LEDs to this range of T_c values showed excellent LFM values, with most DUTs being assigned the minimal α value because the calculated α value was below the permitted threshold. In fact, the LFM values measured for Products COB-2 and COB-3 increased during the 6,000 hrs of testing reported here. This behavior is indicative of an efficiency increase that sometimes occurs during the early stages of LED operation [21]. In previous instances when this behavior occurred, the LFM eventually exhibited exponential decay that lasted for the remainder of the product life.

Although the behavior of the COB LEDs during RTOL tests closely followed that in the previous LM-80 study, the behavior during the 75OL tests was different. Because the 75OL tests were conducted in an environmental chamber with air circulation, the difference between the heat sink temperature and the ambient temperature was less than during the RTOL tests. As a result, the T_c values measured for these devices ranged between 85°C and 108°C, as shown in **Table 2-4**, which is similar to the T_c values measured during the RTOL tests. Despite the small difference in T_c values between the RTOL and 75OL tests, the α values during the 75OL tests were approximately an order of magnitude higher, which suggests that the DUTs were in a higher state of stress. The cause for this difference in α values is unknown, although one possible explanation is an increase in the thermal resistance (Θ_{cs}) between the case and the heat sink because of degradation of the TIM separating the two. It is possible that other, yet to be identified factors are the causes of the higher stress state and the lower LFM values.

The LFM data suggest that the stress experienced by the DUTs during the 75OL tests was much greater than that experienced by the DUTs during the RTOL test; however, the chromaticity shift behavior between the

DUTs in the two tests was analogous. As shown in **Appendix D**, the chromaticity shift direction was generally similar for DUTs during the RTOL and 75OL tests, but the chromaticity shift magnitude was clearly larger during the 75OL tests, consistent with a higher state of stress. The chromaticity shift for Products COB-2 and COB-5 proceeded at a relatively constant rate throughout the 75OL tests, and the direction of the shift was between that expected for a pure CSM-1 and CSM-2 shift. The chromaticity shift observed for Product COB-3 (cool) was also relatively constant throughout all test periods but proceeded in the generally blue direction, which is indicative of CSM-1 behavior. In contrast, both COB-3 (warm) exhibited an initial shift in the green direction (CSM-2), followed by a shift that was intermediate between the blue and green directions. This behavior is consistent with the earlier reports that there are three main chromaticity shift behaviors for COB LEDs: pure CSM-1 behavior (i.e., blue shift), pure CSM-2 behavior (i.e., green shift), and a shift between the two [8]. It is unknown whether this third chromaticity shift mechanism is indicative of a new CSM that occurs in the COB LED package or whether it is indicative that both CSM-1 and CSM-2 are occurring simultaneously.

Another way to track chromaticity changes in LED devices is to monitor the change in measured CCT values with test duration. In general, the CCT values of the COB LED DUTs examined during this study increased at a consistent rate throughout the test period. The change in CCT value can be fit with a linear model of the form of **Equation 4-1**, which is shown as follows:

$$CCT(t) = (m * t) + b \qquad \text{(Eq. 4-1)}$$

where
$CCT(t)$ = CCT value at time, t
m = Slope or change in the CCT value with time (i.e., $\Delta y/\Delta t$)
b = y-axis intercept of the CCT value, also known as the initial CCT value.

The modeling parameters for the COB LED DUTs examined during the RTOL and 75OL tests, as well as the correlation coefficient (R^2), are presented in **Table 4-2**.

Table 4-2: Parameters for linear models of CCT change during the RTOL and 75OL tests.

Product	RTOL			75OL		
	m (K/hr)	*B* (K)	R^2	*M* (K/hr)	*B* (K)	R^2
COB-2	0.008	2,729	0.76	0.020	2,725	0.95
COB-3 (warm)	0.003	2,748	0.65	0.012	2,744	0.91
COB-3 (neutral)	0.005	4,289	0.18	0.059	4,207	0.88
COB-3 (cool)	0.011	6,889	0.13	0.180	6,600	0.83
COB-5	0.014	2,731	0.83	0.018	2,717	0.93

The slope of CCT change was positive for all DUTs, and this rate of change was higher for the DUTs during 75OL tests than for the DUTs during RTOL tests. This finding is consistent with the chromaticity shift data. In addition, the high correlation coefficients (i.e., R^2) observed for most models are suggestive of consistent changes in CCT values throughout the experimental tests. Therefore, while the 75OL DUTs may have experienced a higher level of stress resulting in α values higher than the RTOL DUTs, the self-consistency of the data sets between RTOL and 75OL tests and their agreement with behaviors observed for earlier COB LED products in LM-80 data suggest that 75OL conditions did not cause any new failure modes. Instead, the 75OL test appeared to have accelerated failure, which is one of the goals of ASTs, for a yet to be identified reason. Because the only parametric failures that have been observed to date during this testing were chromaticity shift failures from Products COB-3 (neutral) and COB-3 (cool), it appears likely that at least some COB LEDs will exhibit parametric failure because of excessive chromaticity shifts.

The Product MS-6 DUTs provide an interesting comparison with the COB LEDs. Product MS-6 contains two separate circuits, each with one LED die that is mounted on an Ag-plated Cu lead frame. The lead frame is encased in a heat-resistant polymer, thought to be epoxy molding compound, that serves as a white diffuse reflector for radiation from the LEDs. The size of the LEDs used in Product MS-6 are similar to those used in the COB LED DUTs, but the number of LED die is much higher for the COB LEDs than Product MS-6. The thermal management load was also much lower. The structure of Product MS-6 produced superior luminous efficacy values of up to 162 lm/W, and the radiant efficiency of Product MS-6 reached 0.53 for the cool white setting. In contrast, the luminous efficacies of the COB LEDs were at least 20% lower than Product MS-6, and the maximum radiant efficiency for the COB LED DUTs was 0.44 for Product COB-3 in the cool white setting. Clearly, the higher number of die and wire bonds in COB LEDs are impacting both the radiant efficiency and luminous efficacy of the LED package platform. In addition, the higher thermal management load of the COB package is likely to impact the radiant efficiency and the luminous efficacy that can be produced from the package.

The importance of thermal management in COB LEDs was illustrated by the EQE study on some of the COB DUTs that had been decapped. When operated at the same current density, the EQE of Product COB-4 was practically the same as that of the MP-LED product (i.e., Product MS-6). This high EQE value demonstrates that the EQE of a COB package can be made similar to that of an MP-LED provided that the epitaxy is comparable, the COB package is operated at a less than maximum current density, and adequate thermal management measures are taken. This finding also demonstrates that there are significant opportunities for improving the performance of COB LED packages by addressing light absorption issues and thermal management.

5 Conclusions

The COB LED package platform provides the highest density lighting flux in an LED package that also has the thinnest profile. COB LEDs are formed by interconnecting large numbers of MP-LED die to form a dense LES that is situated directly on an excellent thermal conductive substrate (e.g., MCPCB, ceramic). This report provides initial benchmarks of the performance of selected COB LED products and examines the luminous flux and chromaticity maintenance characteristics of COB LED packages with LESs ranging between 4.5 mm and 14.6 mm. All DUTs examined during this study were mounted on appropriate heat sinks with a TIM between the heat sink and the COB LED. During RTOL tests in still air where the T_c value of the COB LED DUTs was generally below 105°C, the DUTs exhibited excellent LFM performance with most decay rate constants (α in ANSI/IES TM-21-19) assigned to the minimum value of 2.0×10^{-6}. During similar tests in 75OL, where circulating air kept the T_c value between 85°C and 108°C, the α values were significantly higher, indicating that a greater degree of thermal stress was placed upon the DUTs from an unidentified cause, which underscores the need for effective thermal management for these DUTs.

The chromaticity shifts observed for the COB LEDs exhibited one of three characteristics as follows:

- A chromaticity shift in the generally blue direction, indicating that the CSM-1 behavior was observed for higher CCT DUTs
- A chromaticity shift in the generally green direction, indicating that the CSM-2 behavior was observed for many of the lower CCT DUTs
- A chromaticity shift that is between the generally green and generally blue directions, suggesting that both CSM-1 and CSM-2 behaviors are happening simultaneously, was found in some lower CCT DUTs.

Despite the higher stress conditions during the 75OL test, the general chromaticity shift directions were similar during RTOL and 75OL tests; only the magnitude of the chromaticity shift was higher during the 75OL test. The similarity in chromaticity shift direction between RTOL and 75OL indicates that the 75OL test conditions of the 75OL tests did not create a new failure mechanism because the chromaticity shift was unchanged.

Instead, the 75OL test accelerated both luminous flux decay and chromaticity shift and resulted in several parametric failures for excess chromaticity shift (i.e., $\Delta u'v' \geq 0.007$).

Together, these findings indicate that COB LEDs are an emerging LED packaging platform that can provide luminous efficacies of more than 100 lm/W in a small, thin profile package that is suitable for downlights, spotlights, and other high light intensity applications. However, the efficiency of COB LEDs is generally lower than MP-LEDs because of the large number of absorbing materials (e.g., die, wire bonds, reflectors) in the LES and the large amount of waste heat that is produced in a small area. Both of these technical challenges to efficiency are opportunities to improve the efficiency of COB LEDs. This study clearly demonstrated the importance of thermal management in achieving long operational lifetimes from COB LEDs. Thermal degradation of the COB LED package or the TIM between the COB package and the heat sink can cause issues, such as corrosion of the Ag reflectors, darkening of the silicone matrix, or other temperature-induced effects, which can cause rapid loss of luminous flux and chromaticity shifts. Therefore, it is anticipated that COB LEDs will evolve in new ways to provide additional capabilities to SSL products.

References

1. Lighting Manufacturer. (N.D.). *Best COB LEDs: Chip-on-board LED packages*. Retrieved from https://www.manufacturer.lighting/info/195/#:~:text=A%20chip%2Don%2Dboard%20(,polymer%20containing%20a%20yellow%20phosphor.

2. Mehr, Y., Bahrami, A., van Driel, W. D., Fan, X. J., Davis, J. L., & Zhang, G. Q. (2020). Degradation of optical materials in solid-state lighting systems. *International Materials Reviews, 65*(2), 102–128. https://doi.org/10.1080/09506608.2019.1565716

3. Wu, H.-H., Lin, K.-H., & Lin, S.-T. (2012). A study on the heat dissipation of high power multi-chip COB LEDs. *Microelectronics Journal, 43*, 280–287. doi:10.1016/j.mejo.2012.01.00

4. Next Generation Lighting Industry Alliance and LED Systems Reliability Consortium. (2019, July). *Dim-to-warm LED lighting: Initial benchmarks*. Retrieved from https://www.nglia.org/documents/LSRC_Dim-to-Warm_Paper_final_073019r.pdf

5. Rountree, K., Davis, L., McCombs, M., Pope, R., Kim, J., Mills, K., & Hansen, M. (2020, January). *Dim-to-warm LED lighting: Stress testing results for select products*. U.S. Department of Energy, Washington, DC. Retrieved from https://www.energy.gov/sites/prod/files/2020/04/f73/ssl-d2w-led-stress-testing-2020.pdf

6. Business Wire. (2020, April 13). *Chip-on-board (COB) LED market 2019 2023: Growing adoption of COB LED in smart lighting to boosts growth: Technavio*. Retrieved from https://www.businesswire.com/news/home/20200412005005/en/Chip-on-Board-COB-LED-Market-2019-2023-Growing-Adoption-Of-COB-LED-in-Smart-Lighting-to-Boost-Growth-Technavio

7. DOE (U.S. Department of Energy) BTO (Building Technologies Office) Lighting R&D (Research and Development) Program. (2020, January). *2019 Lighting R&D opportunities.* U.S. Department of Energy, Washington, DC. Retrieved from https://www.energy.gov/sites/prod/files/2020/01/f70/ssl-rd-opportunities2-jan2020.pdf

8. Davis, J. L., & Hansen, M. (2020, March). *Lumen and chromaticity maintenance behavior of light-emitting diode (LED) packages based on LM-80 data*. U.S. Department of Energy, Washington, DC. Retrieved from https://www.energy.gov/sites/prod/files/2020/03/f73/rti_lm-80-white-leds_mar2020.pdf

9. Davis, L., Rountree, K., McCombs, M., Mills, K., & Pope, R. (2020). *Changes in SSL device efficiency and optical performance under accelerated aging conditions*. U.S. Department of Energy, Washington, DC. Retrieved from https://www.energy.gov/sites/prod/files/2020/08/f77/ssl-rti-device-efficiency-jun2020.pdf

10. Davis, L., Rountree, K., Mills, K., Pope, R., McCombs, M., and Hegarty-Craver, M. (January 2021). *Changes in SSL device efficiency and optical performance with aging: Final report*. U.S. Department of Energy, Washington, DC.

11. Digi-Key Electronics. (2015). Technical brief: Wakfefield-Vette. *Heat sink design facts & guidelines for thermal analysis*. Retrieved from https://www.digikey.com/en/pdf/w/wakefield-thermal-solutions/heat-sink-design-for-thermal-analysis

12. ANSI (American National Standards Institute) and IES (Illuminating Engineering Society) (2019). *ANSI/IES LM-79-19: Approved method: Optical and electrical measurements of solid-state lighting products*. New York, NY: IES.

13. ANSI (American National Standards Institute) and IES (Illuminating Engineering Society) (2018). *ANSI/IES TM-30-18: IES method for evaluating light source color rendition.* New York, NY: IES.

14. ANSI (American National Standards Institute)/IES (Illuminating Engineering Society) LS-1-20. (2020). *Lighting science: Nomenclature and definitions for illuminating engineering*. Retrieved from https://www.ies.org/standards/definitions/

15. IES (Illuminating Engineering Society). (2019). *IES TM-21-19: Project long-term lumen, photon, and radiant flux maintenance of LED light sources*. New York, NY: IES.

16. Next Generation Lighting Industry Alliance and the LED (Light-Emitting Diodes) Systems Reliability Consortium. (2017, April). *LED luminaire reliability: Impact of color shift*. Retrieved from https://www.nglia.org/pdfs/lsrc_colorshift_apr2017r.pdf

17. Davis, J. L., Young. J., & Royer M. (2016, February). *CALiPER Report 20.5: Chromaticity shift modes of LED PAR38 lamps operated in steady-state conditions.* Retrieved from https://www.energy.gov/sites/prod/files/2016/03/f30/caliper_20-5_par38.pdf

18. Davis, J. L., Mills, K., Yaga, R., Johnson, C., Hansen, M., & Royer. M. (2017). Chromaticity maintenance in LED devices. In *Solid State Lighting Reliability: Components to Systems.* van Driel, W. D., Fan, X., & Zhang, G. Q. (Eds). New York, NY: Springer.

19. Sze, S. M., & Ng, K. K. (2006). LEDs and lasers. *Physics of semiconductor devices.* Pp. 599–662. Wiley: Hoboken, NJ. doi:10.1002/9780470068328.ch12

20. Doane, D. A., & Franzon, P. D. (1993). *Multichip module technologies and alternatives: The basics.* Van Nostrand Reinhold: New York.

21. Bobashev, G., Baldasaro, N., Mills, K., & Davis, J. L. (2016). An efficiency-decay model for lumen maintenance. *IEEE Transactions on Device and Materials Reliability, 16*(3), 277–281.

Appendix A

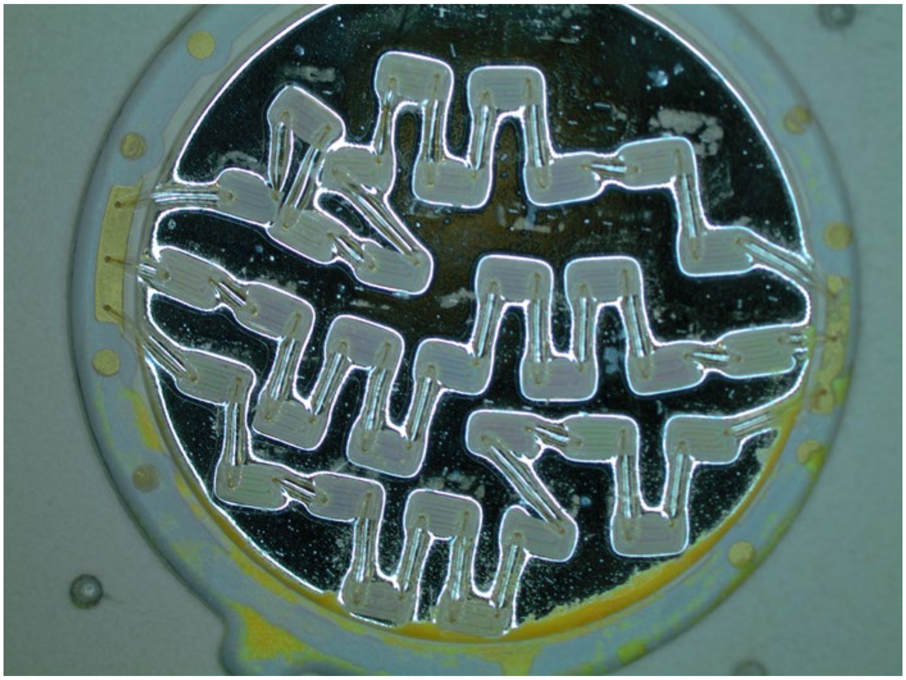

Figure A-1: Image of a decapped Product COB-2.

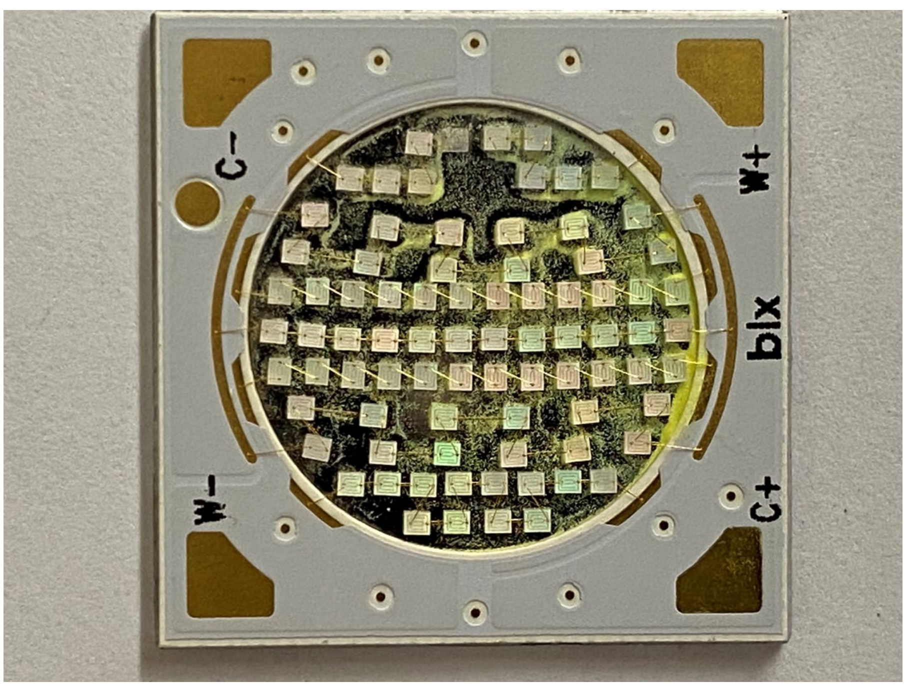

Figure A-2: Image of a decapped Product COB-3.

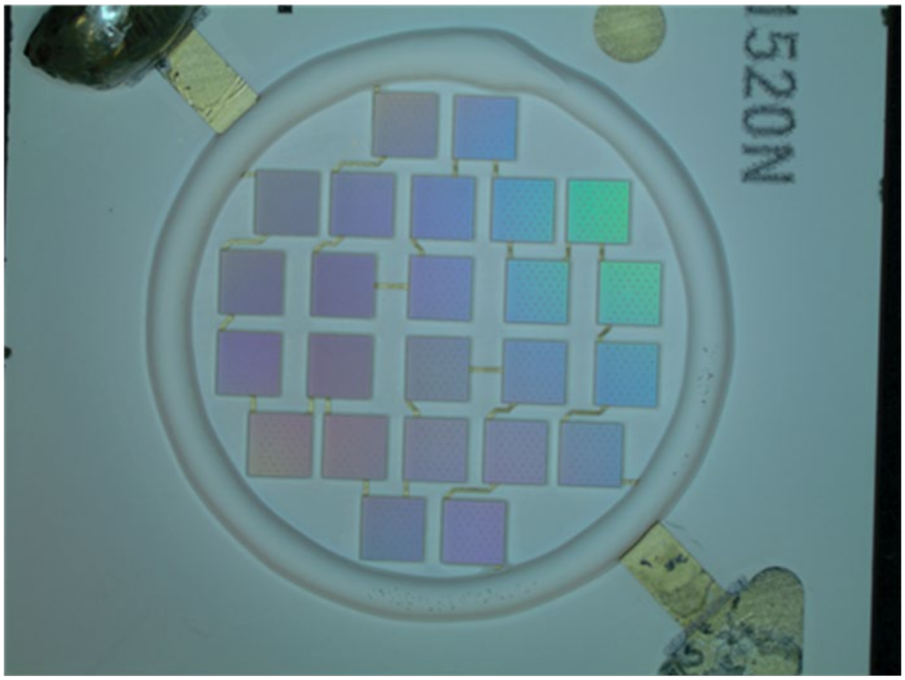

Figure A-3: Image of a decapped Product COB-4.

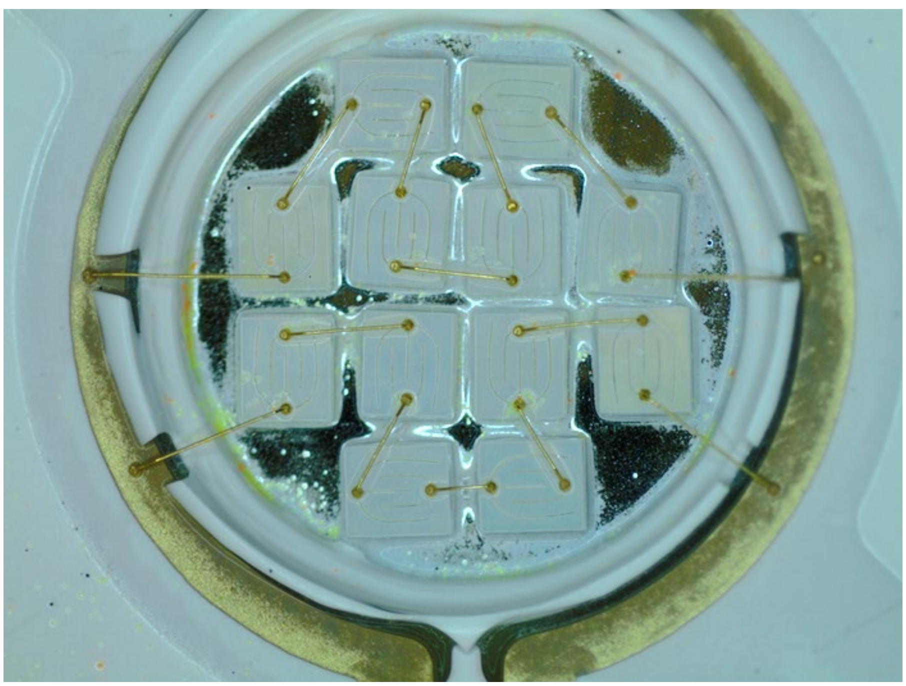

Figure A-4: Image of a decapped Product COB-5.

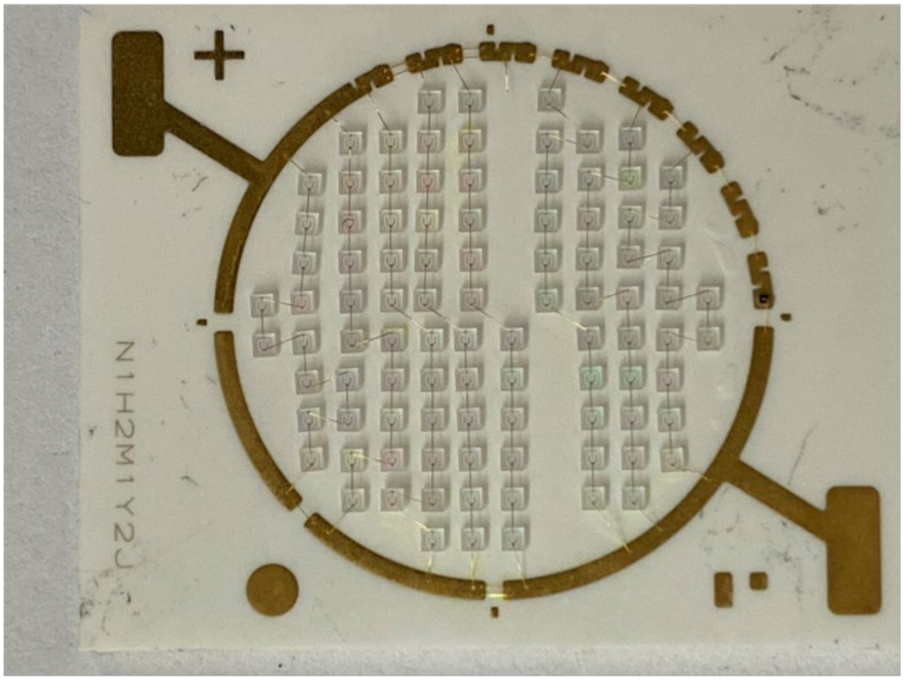

Figure A-5: Image of a decapped Product COB-6. Note: A string of LEDs is missing from the picture.

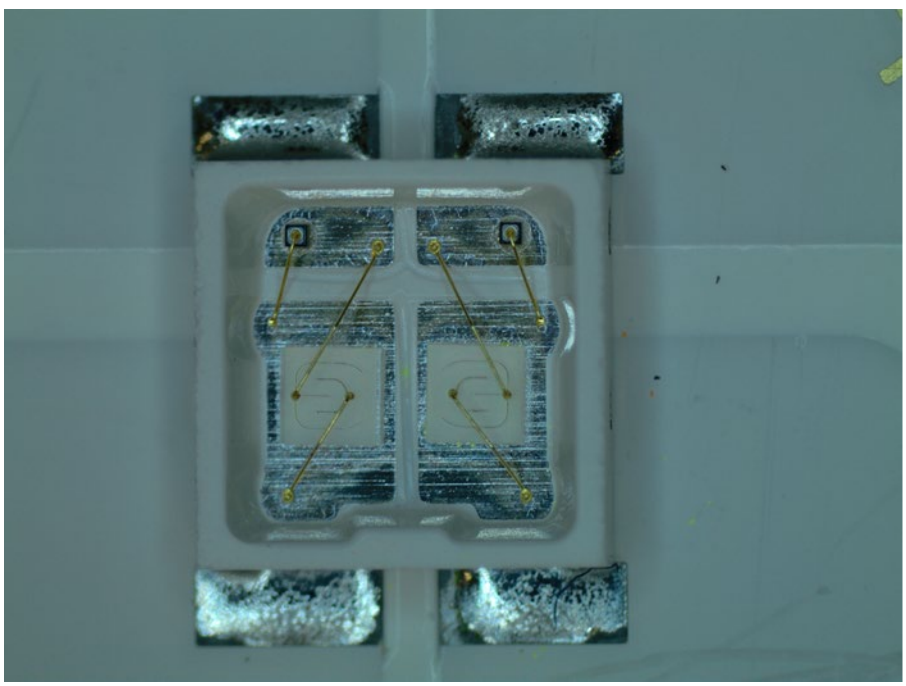

Figure A-6: Image of a decapped Product MS-6.

Appendix B

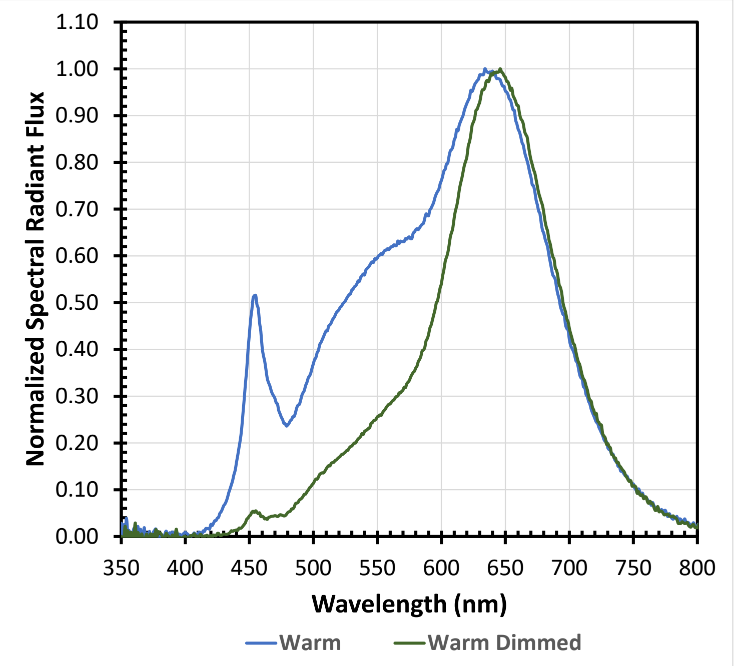

Figure B-1: Normalized spectral power distribution (SPD) of Product COB-1.

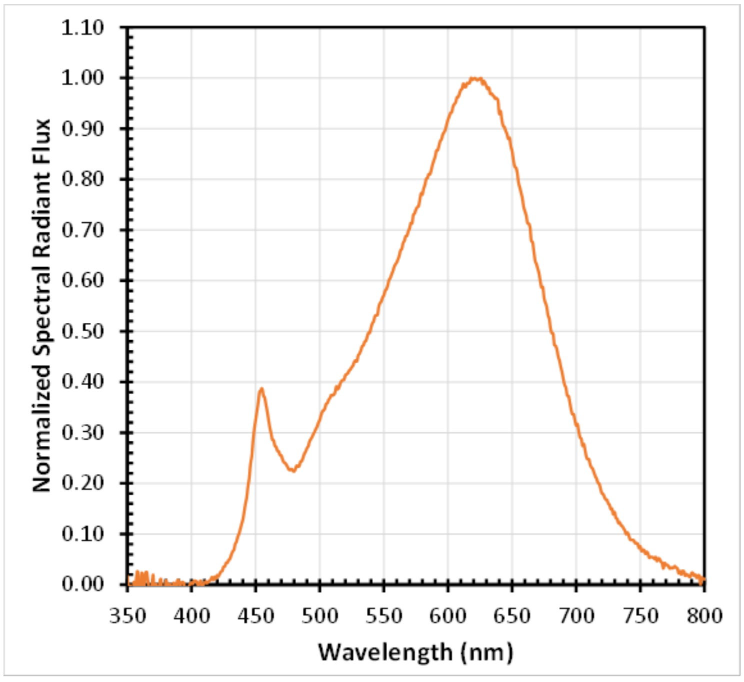

Figure B-2: Normalized SPD of Product COB-2.

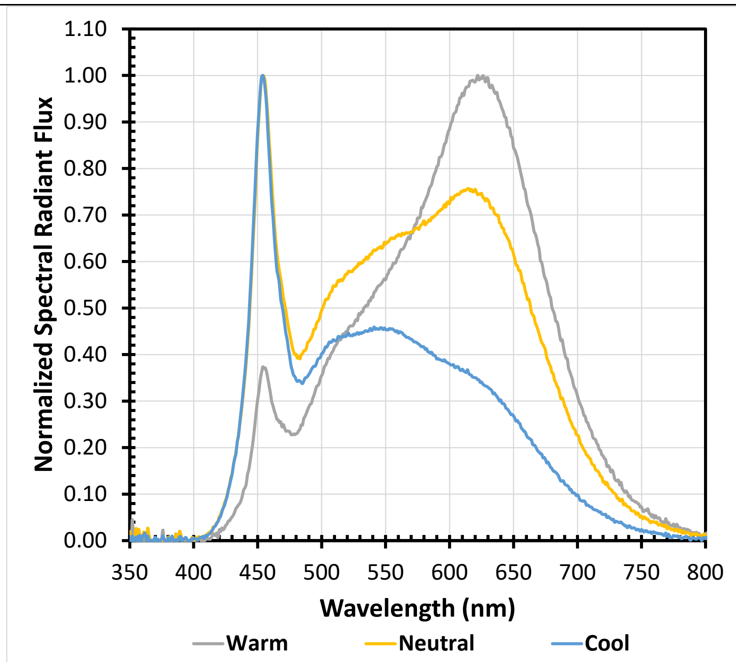

Figure B-3: Normalized SPD of Product COB-3 at the warm white, neutral white, and cool white settings.

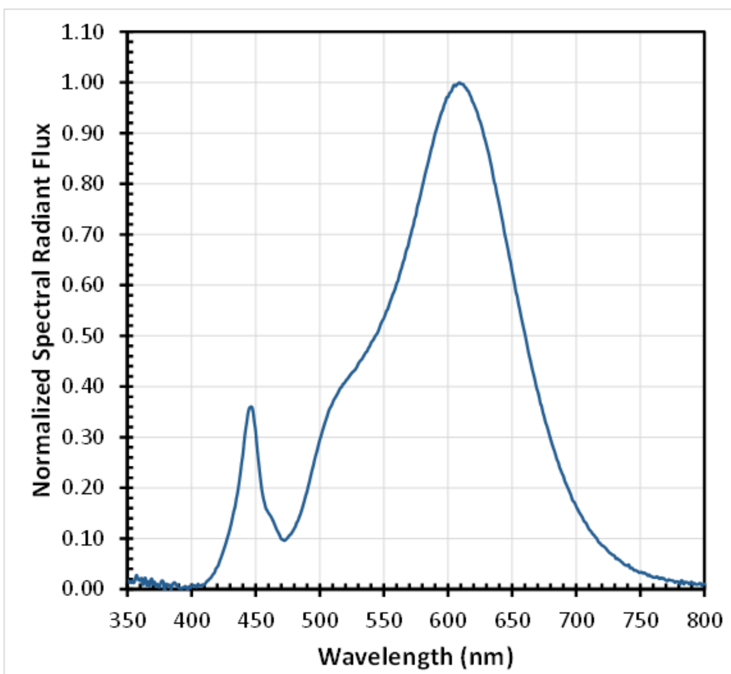

Figure B-4: Normalized SPD of Product COB-4.

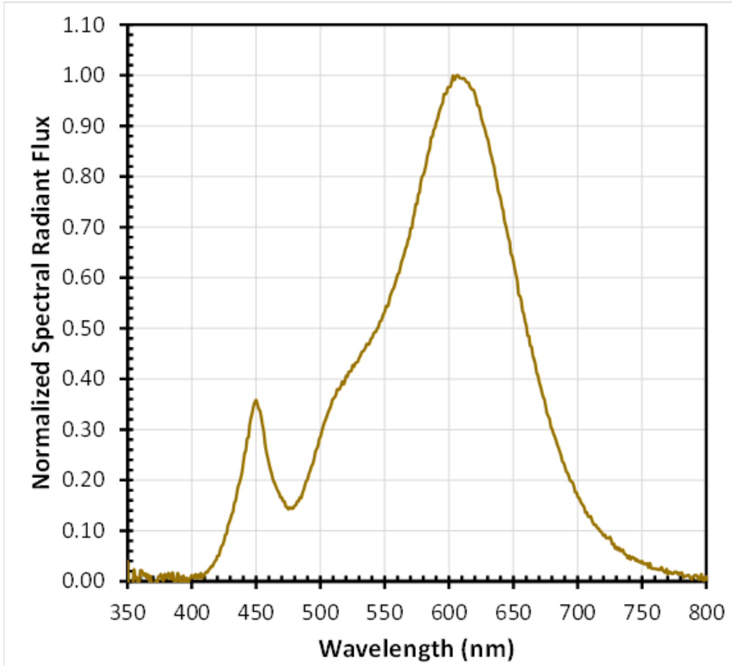

Figure B-5: Normalized SPD of Product COB-5.

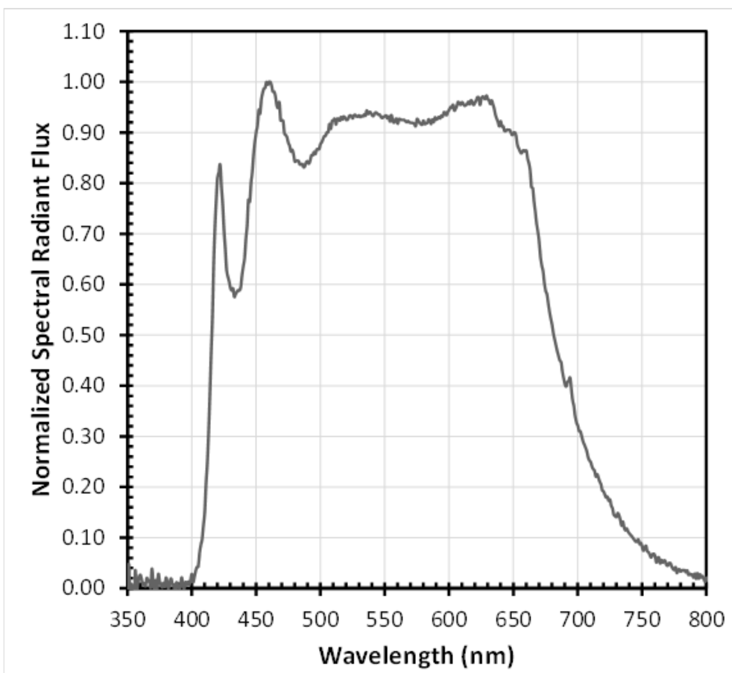

Figure B-6: Normalized SPD of Product COB-6.

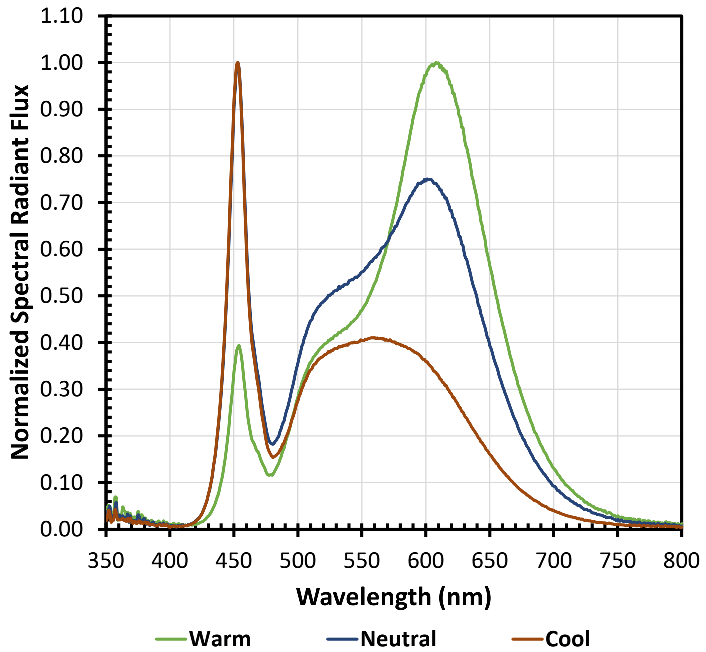

Figure B-7: Normalized SPD of a Product MS-6 DUT at the warm white, neutral white, and cool white settings.

Appendix C

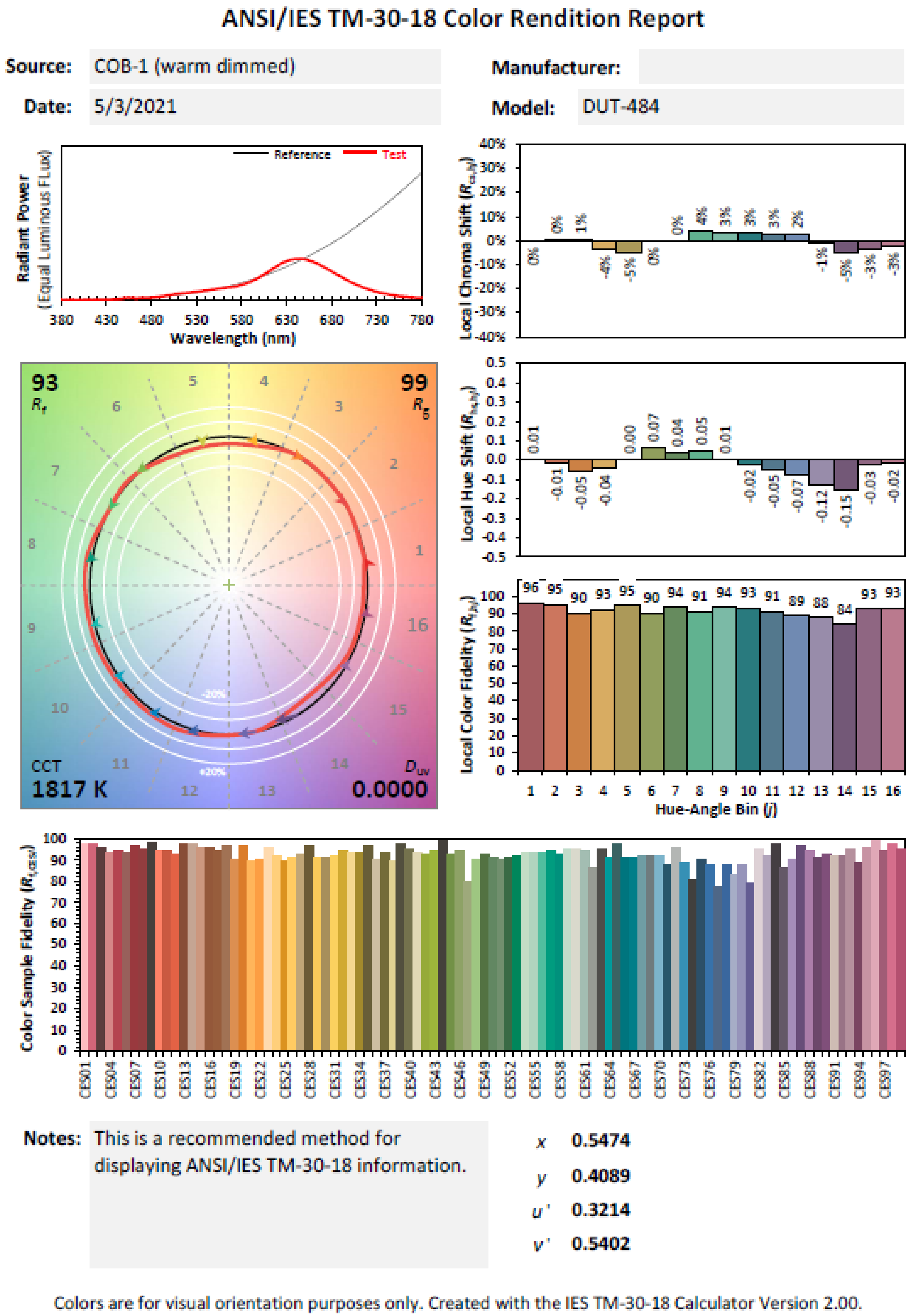

Figure C-1: ANSI/IES TM-30-18 analysis of Product COB-1 in the low power state (warm dimmed).

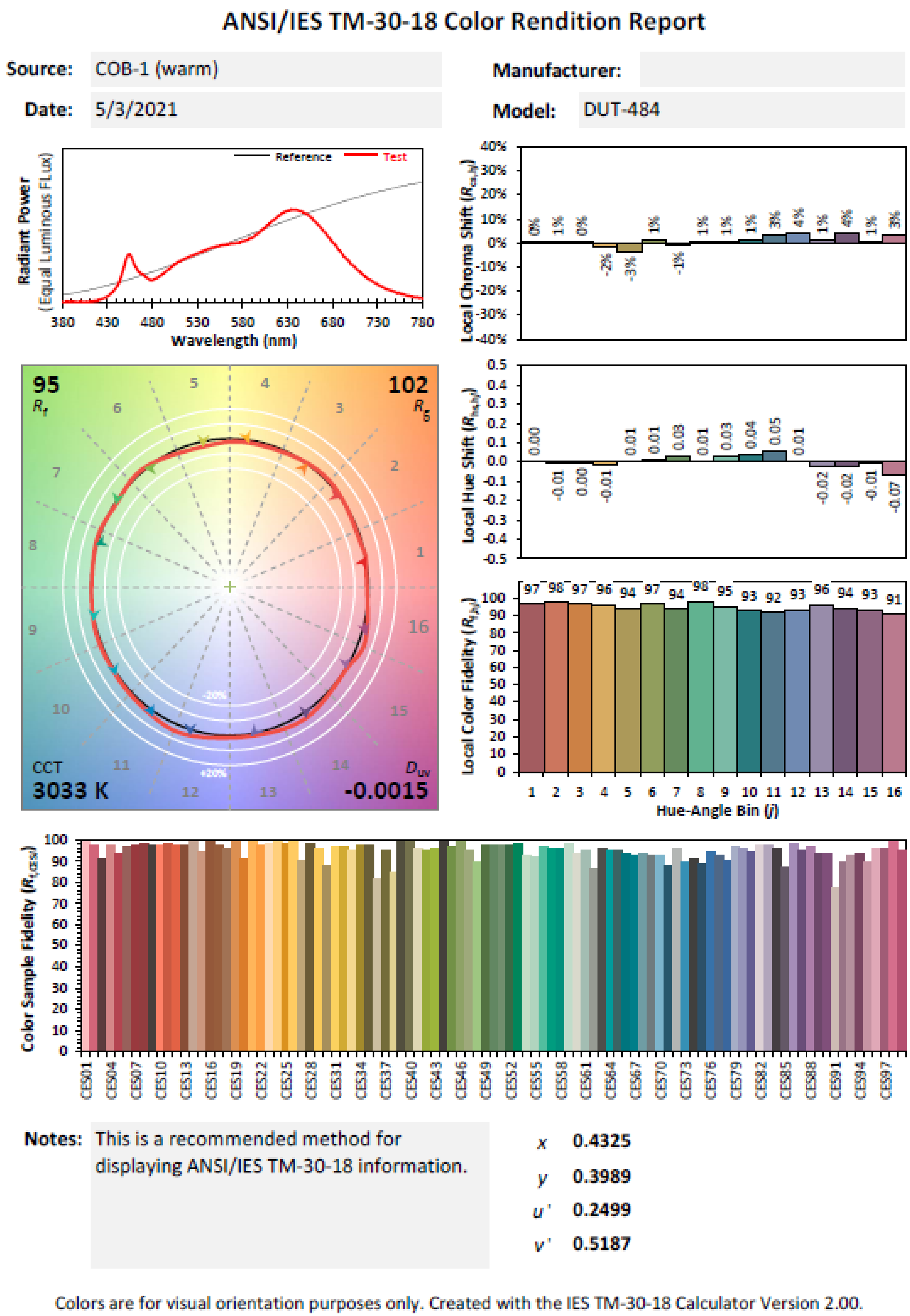

Figure C-2: ANSI/IES TM-30-18 analysis of Product COB-1 in the full power state (warm).

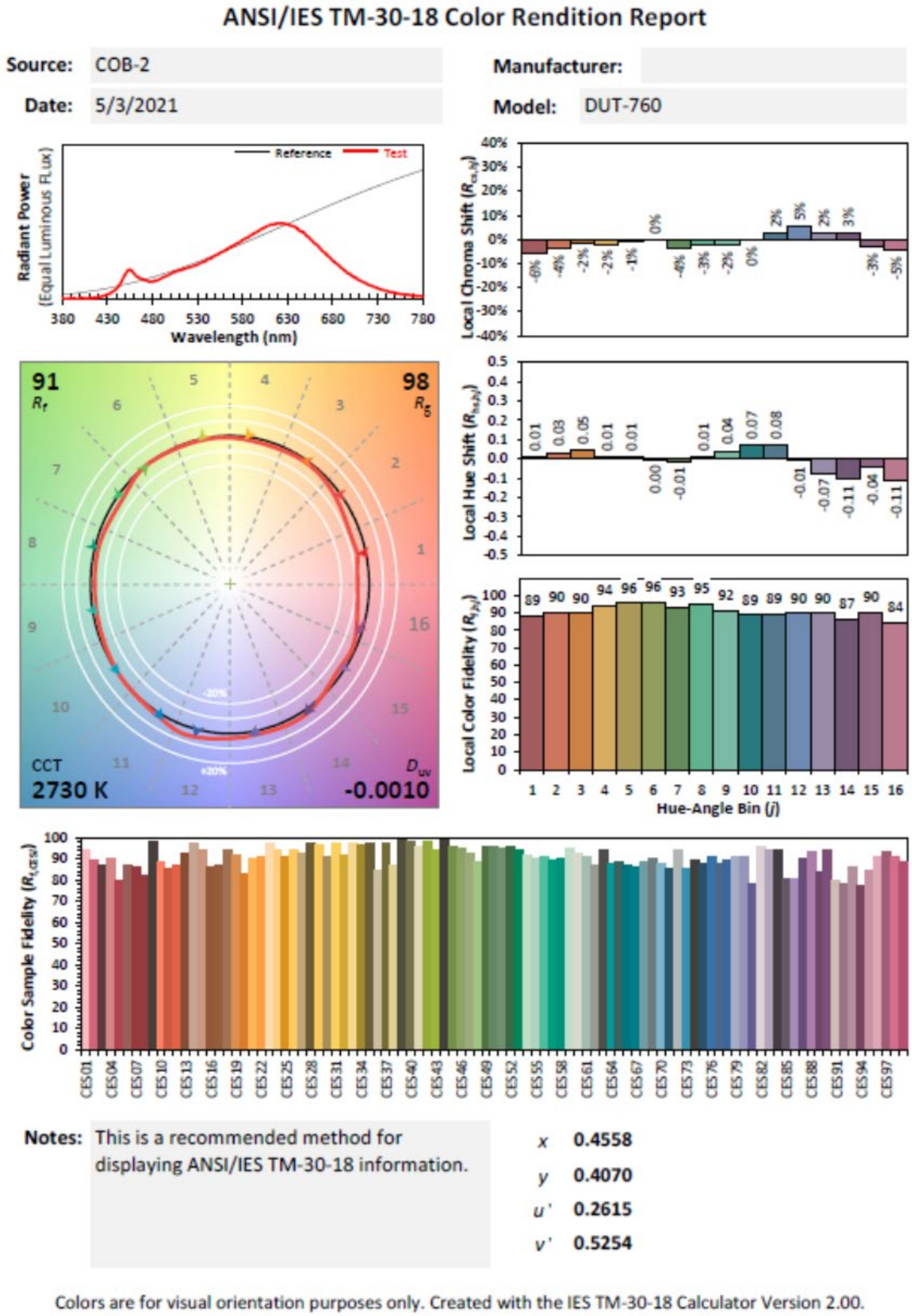

Figure C-3: ANSI/IES TM-30-18 analysis of Product COB-2.

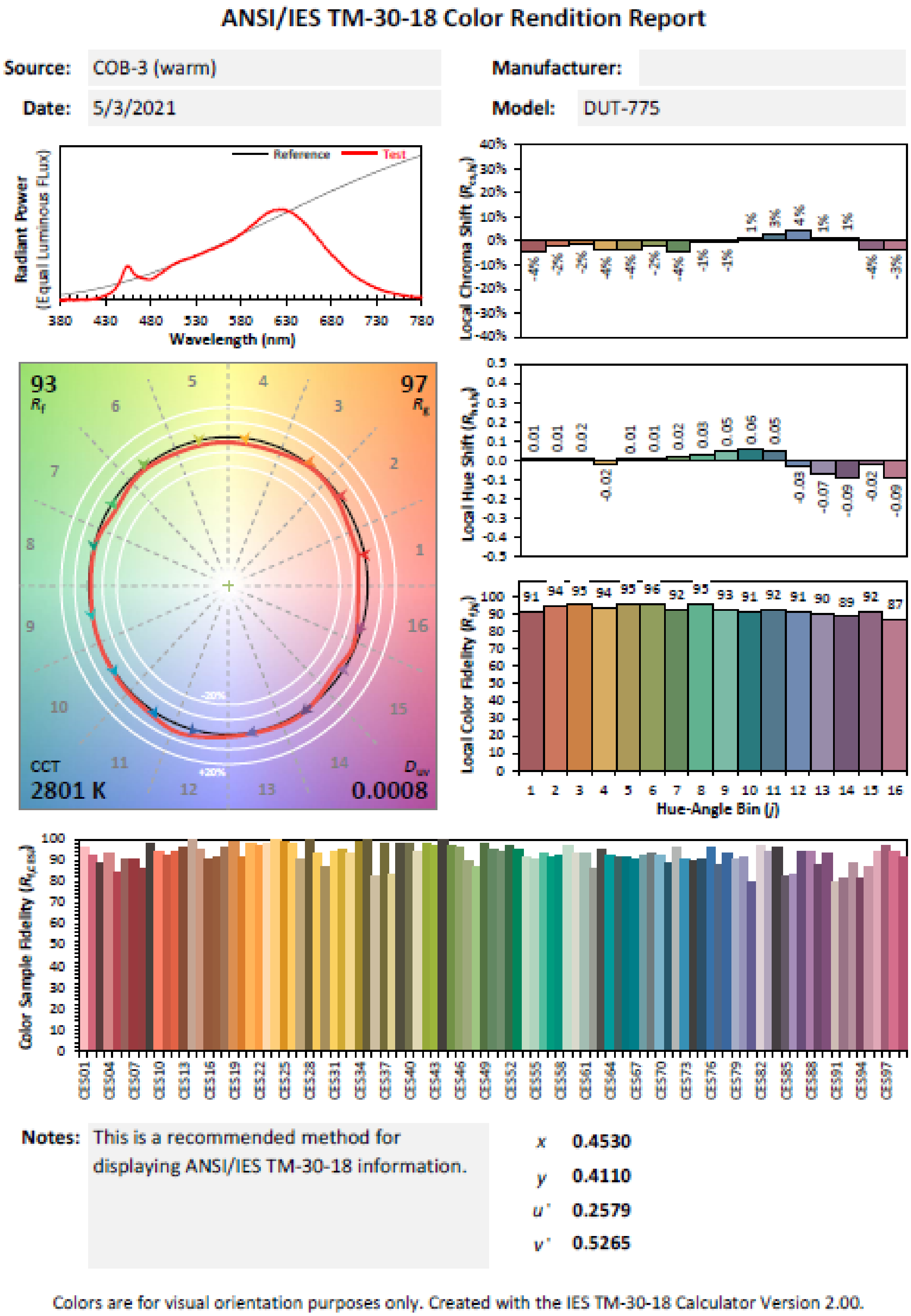

Figure C-4: ANSI/IES TM-30-18 analysis of Product COB-3 at a nominal CCT value of 2,700 K.

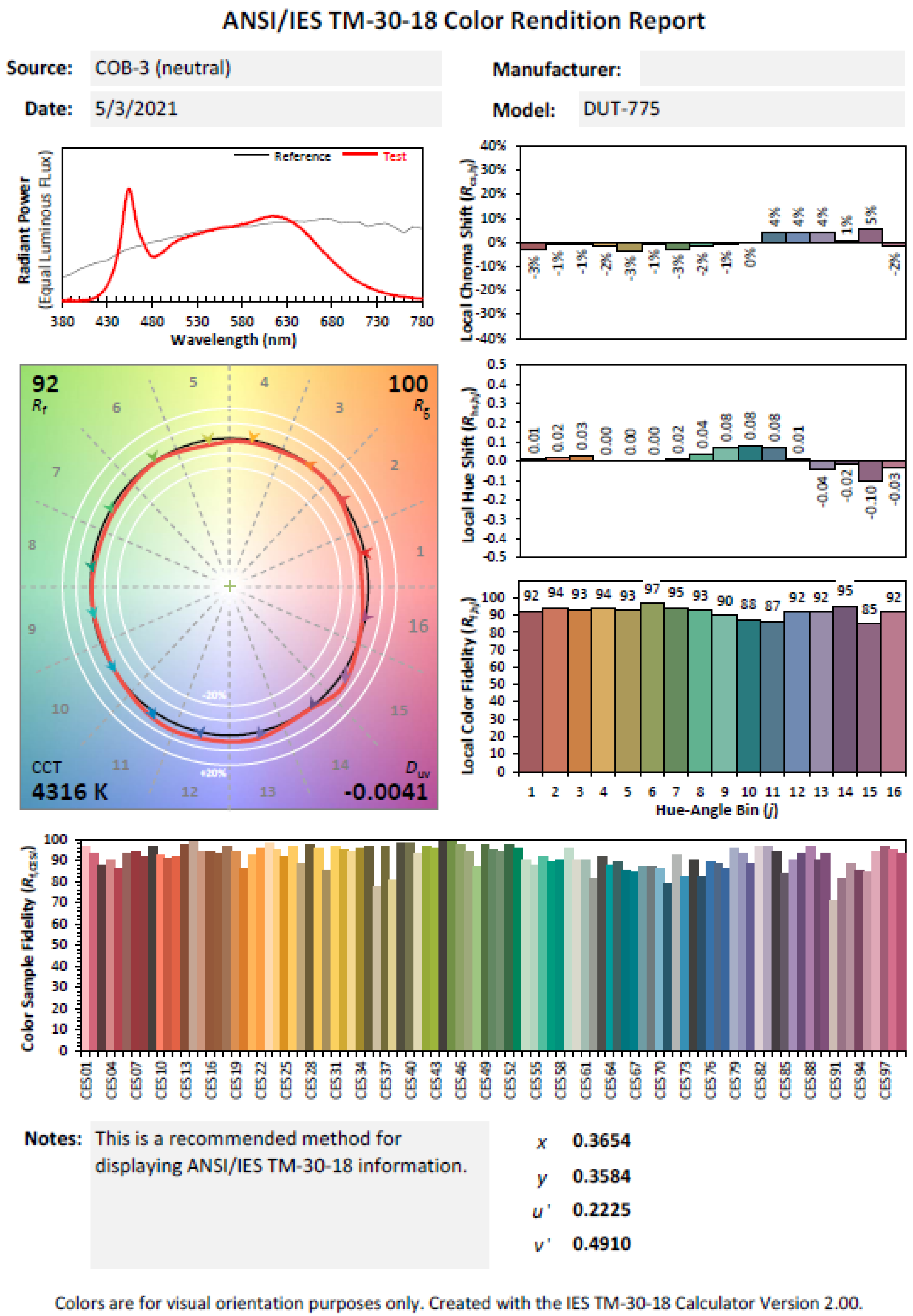

Figure C-5: ANSI/IES TM-30-18 analysis of Product COB-3 at a nominal CCT value of 4,000 K.

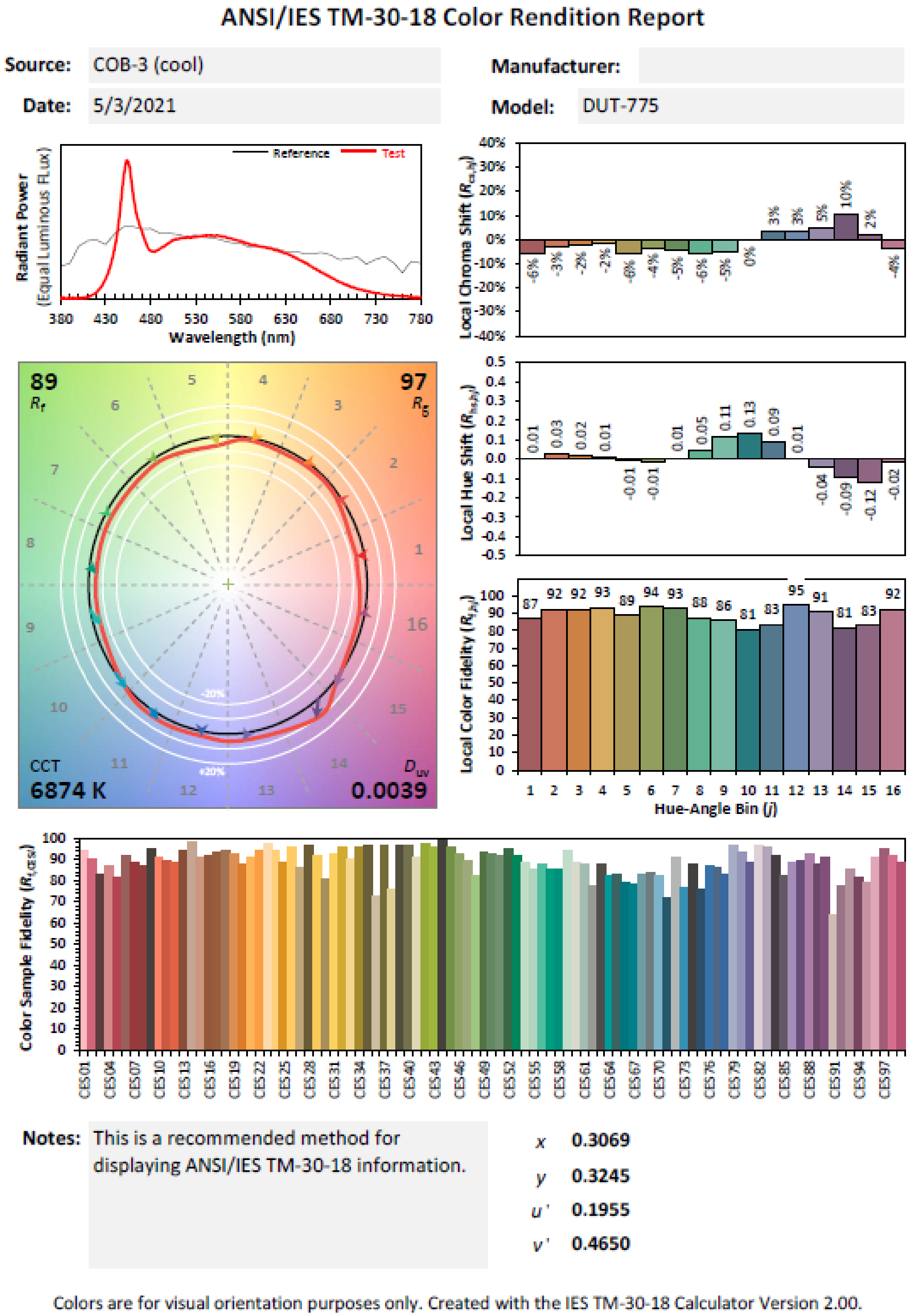

Figure C-6: ANSI/IES TM-30-18 analysis of Product COB-3 at a nominal CCT value of 6,500 K.

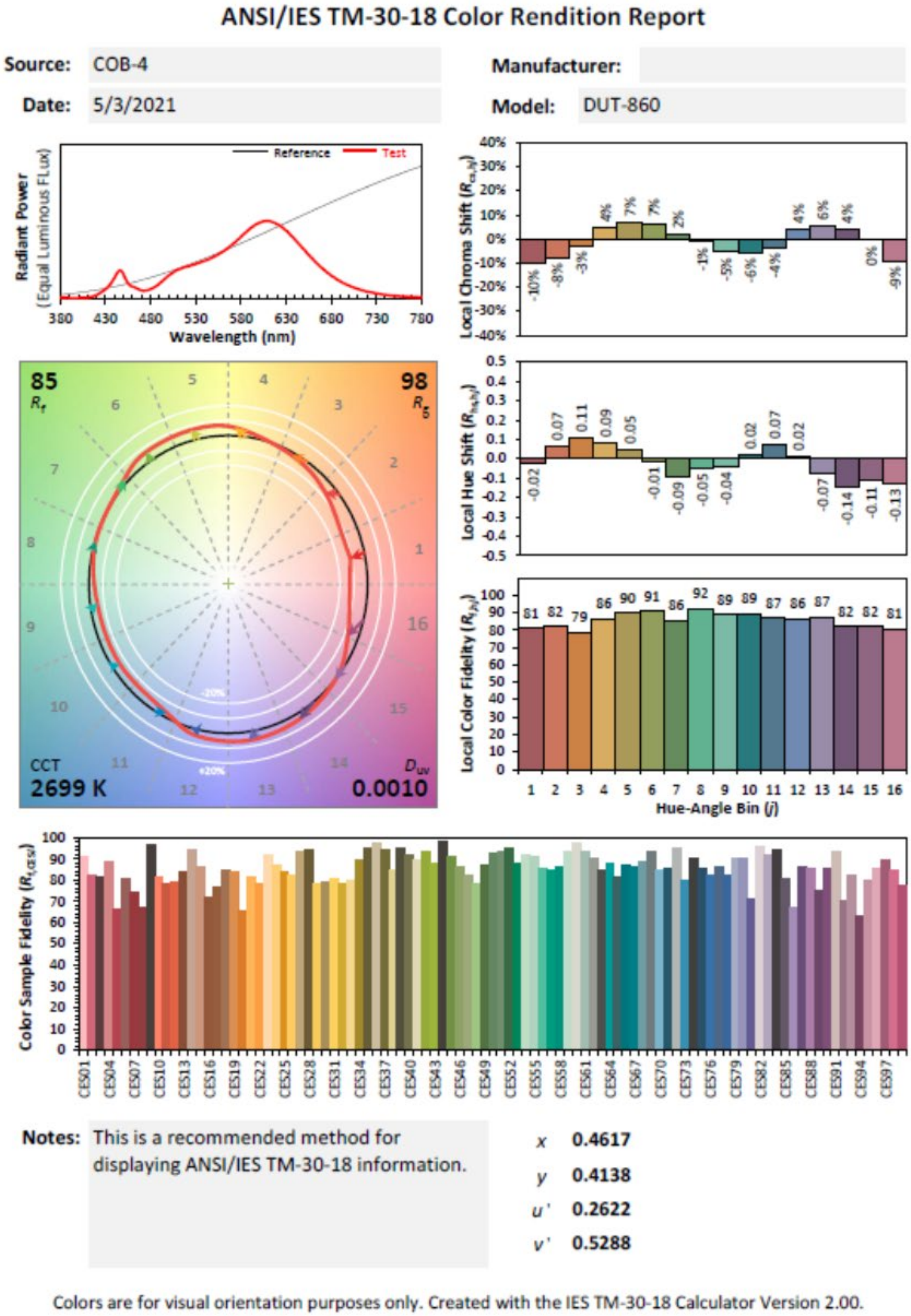

Figure C-7: ANSI/IES TM-30-18 analysis of Product COB-4.

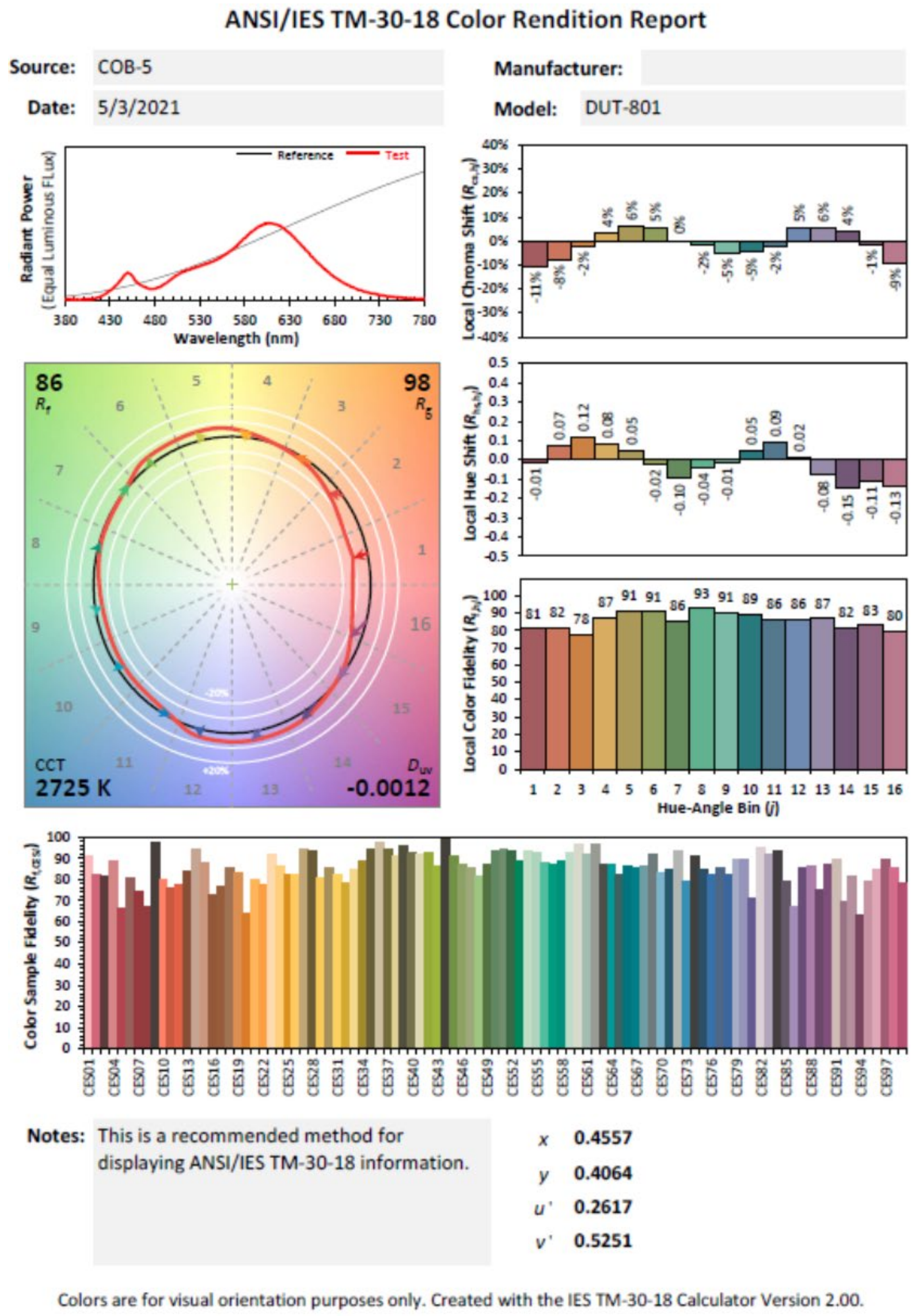

Figure C-8: ANSI/IES TM-30-18 analysis of Product COB-5.

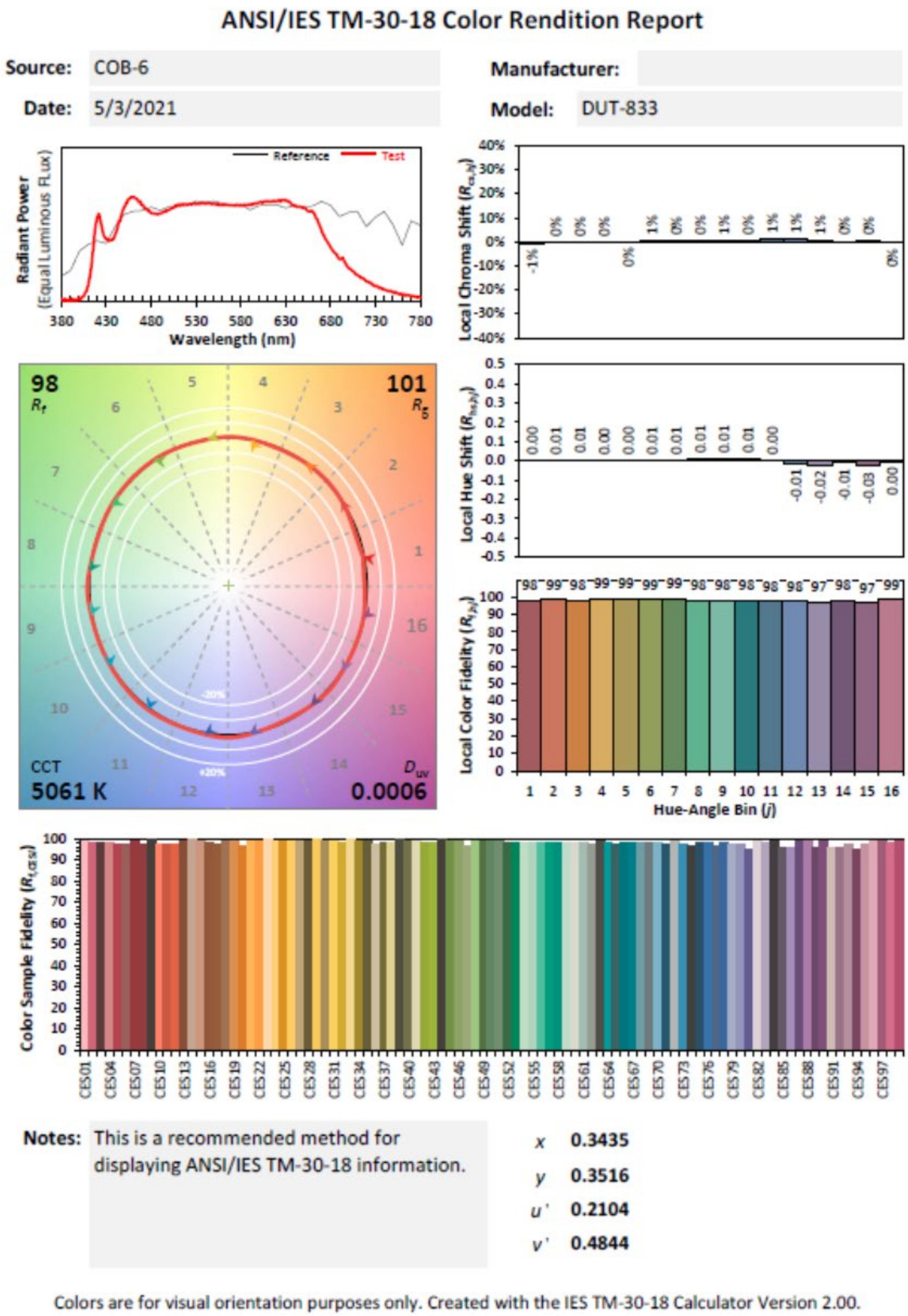

Figure C-9: ANSI/IES TM-30-18 analysis of Product COB-6.

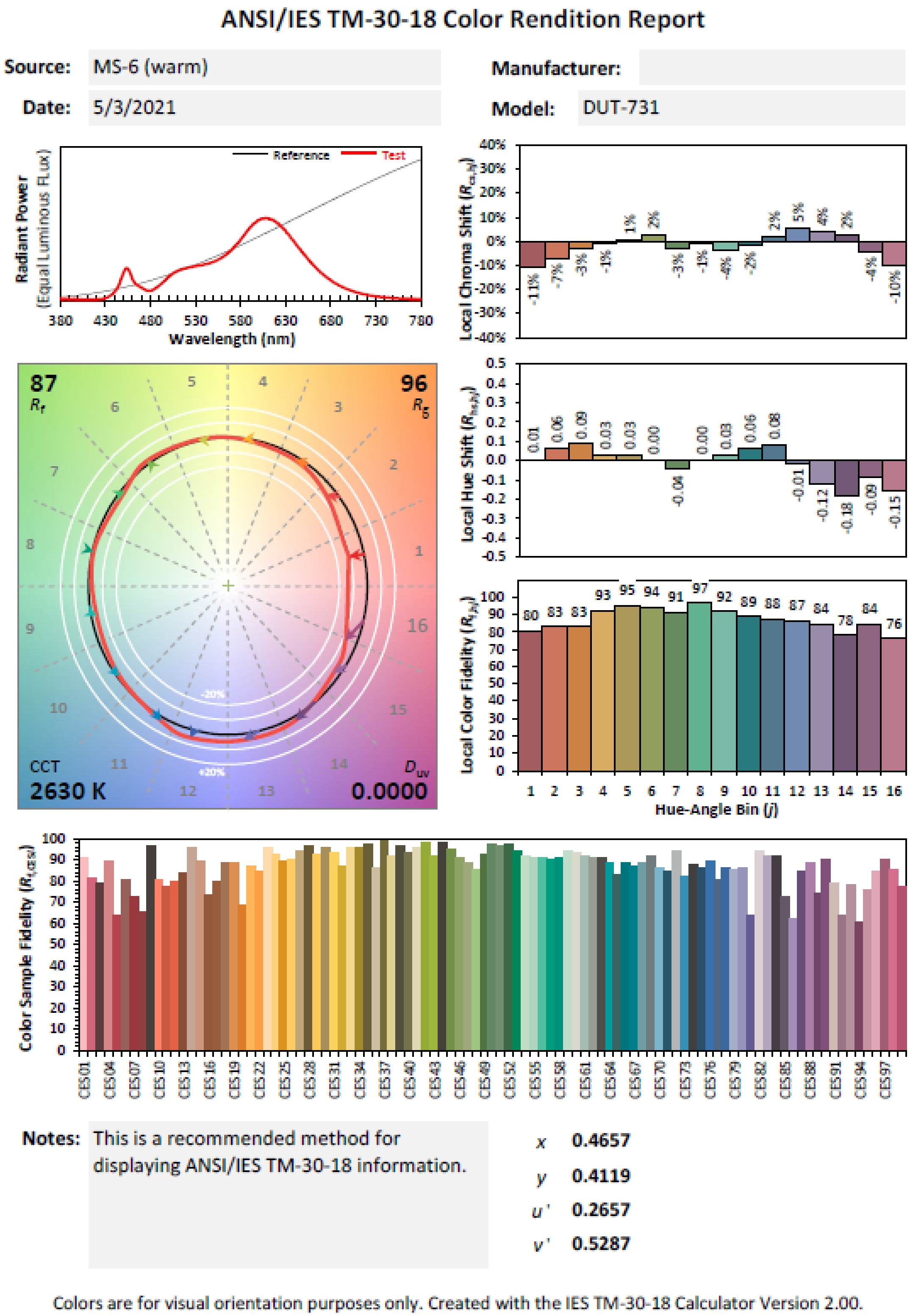

Figure C-10: ANSI/IES TM-30-18 analysis of Product MS-6 taken at a nominal 2.700 K setting.

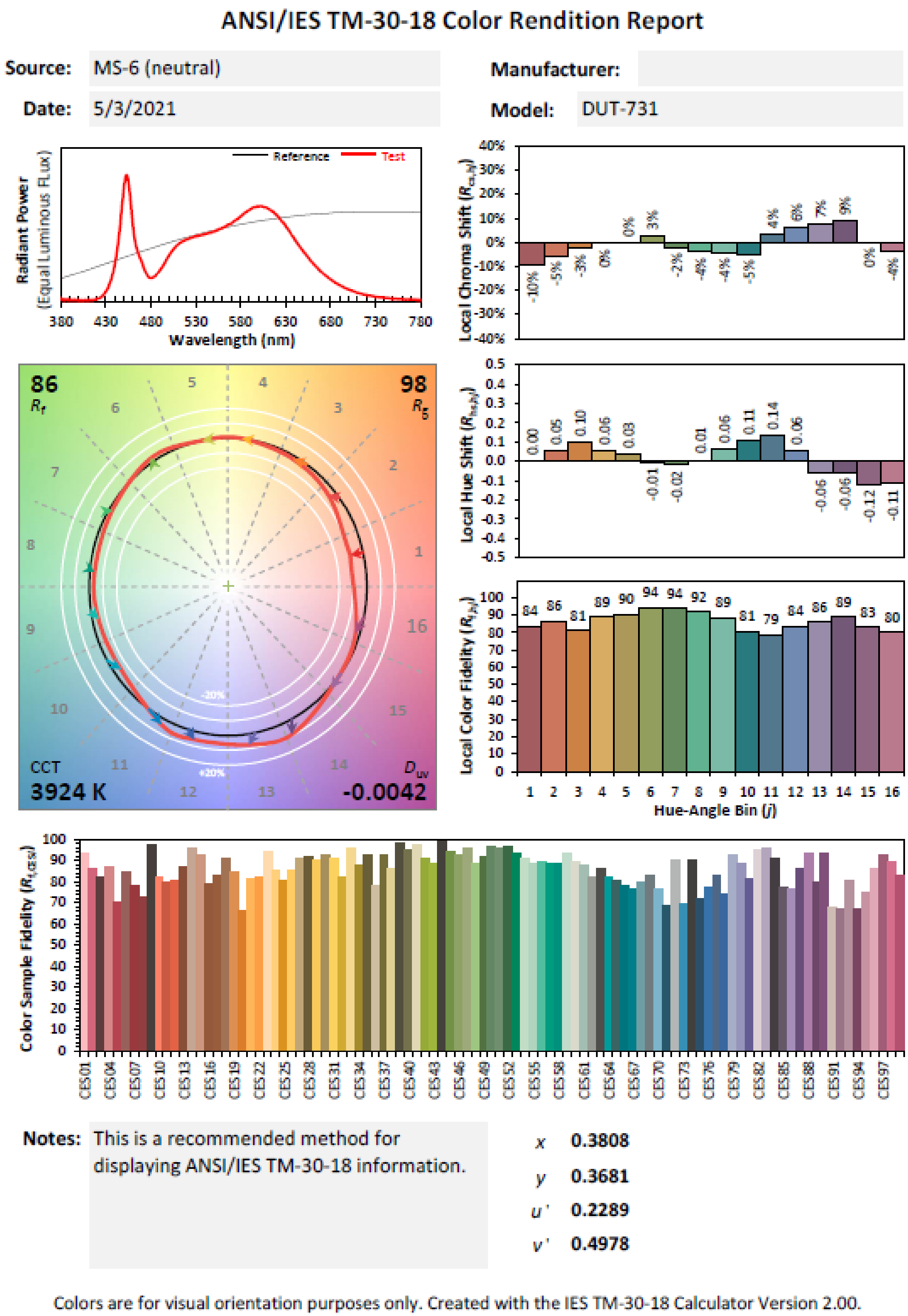

Figure C-11: ANSI/IES TM-30-18 analysis of Product MS-6 taken at a nominal 4,000 K setting.

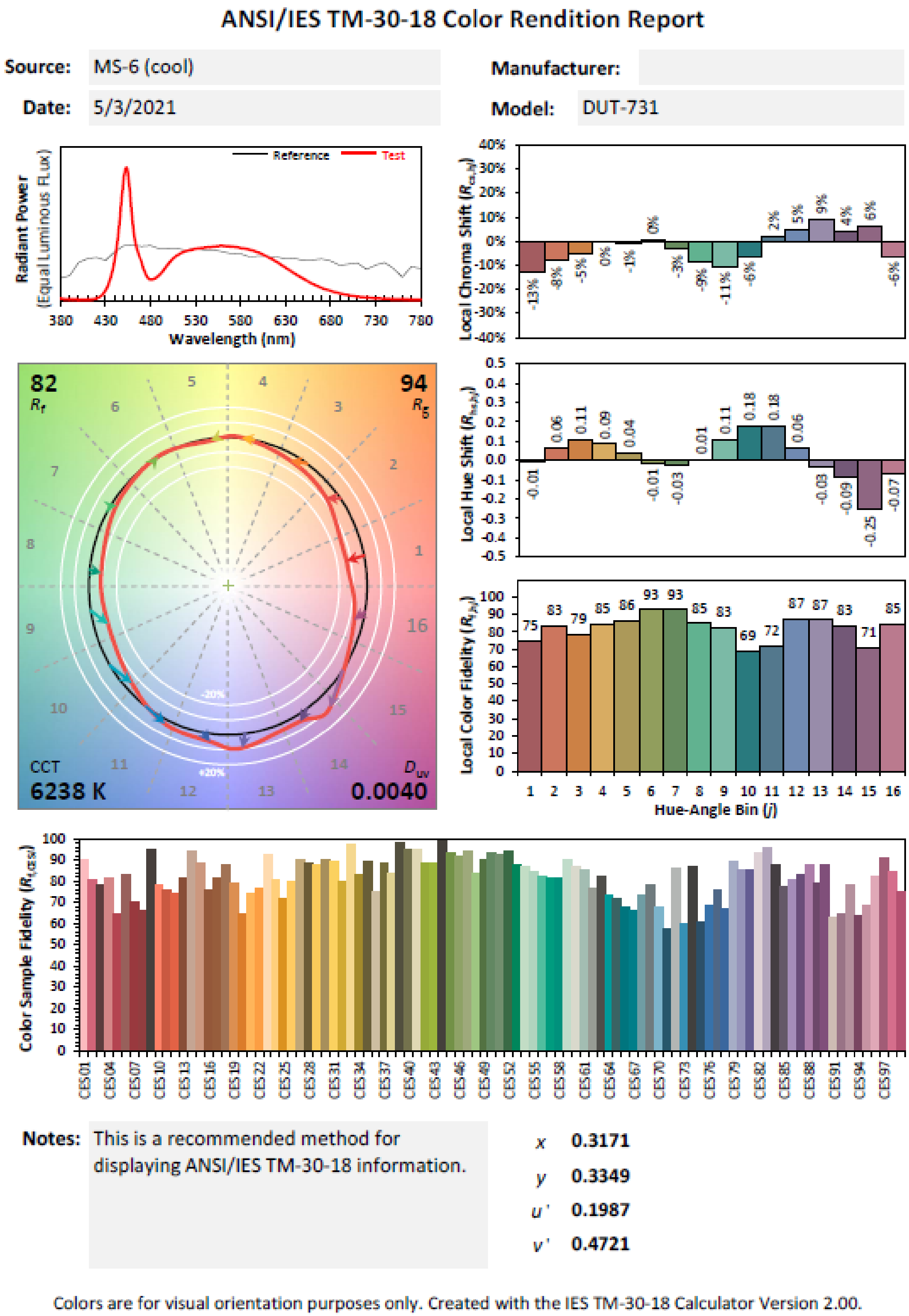

Figure C-12: ANSI/IES TM-30-18 analysis of Product MS-6 taken at a nominal 6,500 K setting.

Appendix D

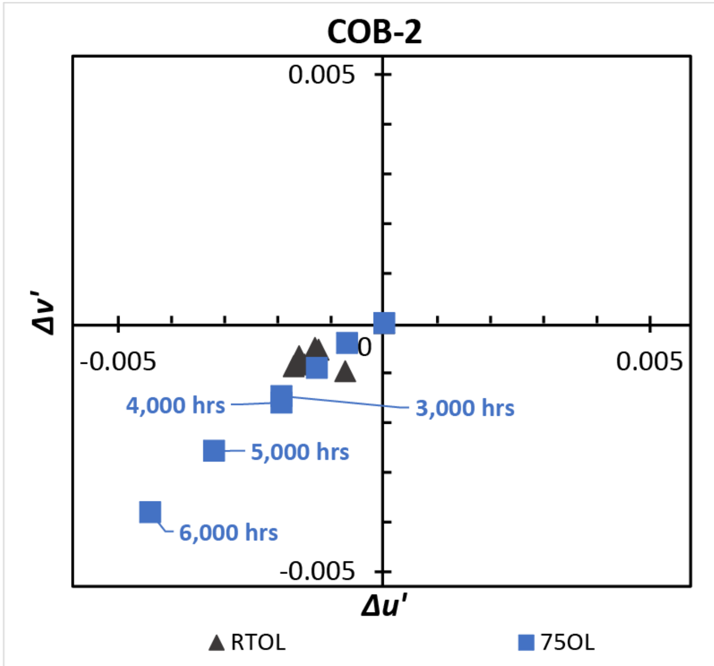

Figure D-1: Chromaticity shift diagram for Product COB-2 during room temperature operating life (RTOL) tests and 75 degree Celsius (°C) operational life (75OL) tests.

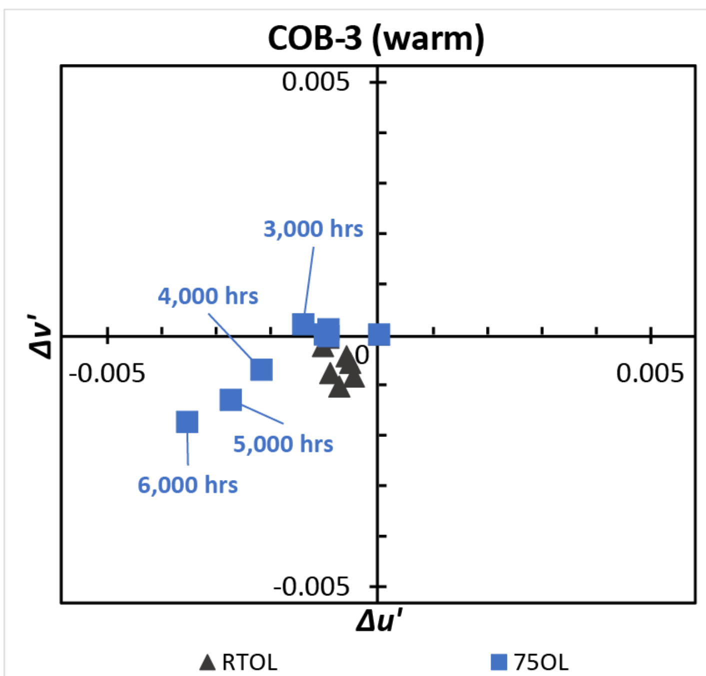

Figure D-2: Chromaticity shift diagram for Product COB-3 (warm) during RTOL and 75OL tests.

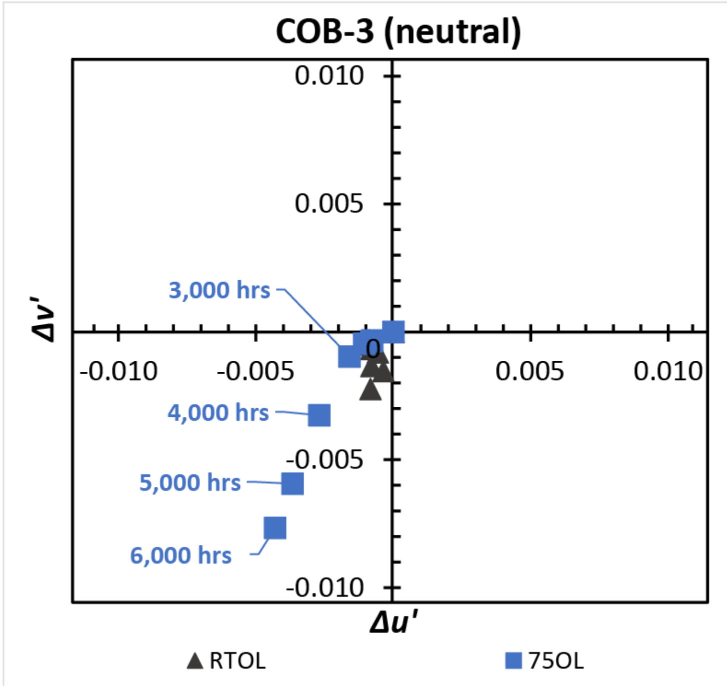

Figure D-3: Chromaticity shift diagram for Product COB-3 (neutral) during RTOL and 75OL tests.

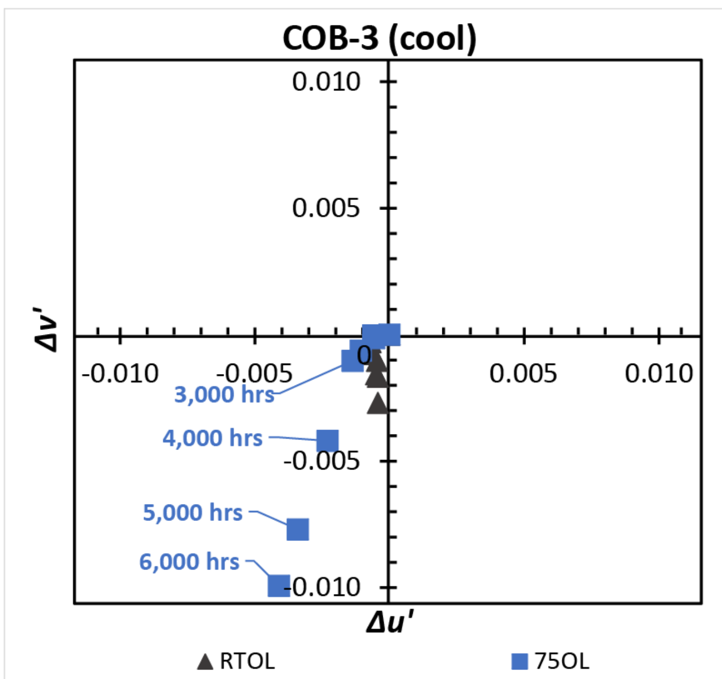

Figure D-4: Chromaticity shift diagram for Product COB-3 (cool) during RTOL and 75OL tests.

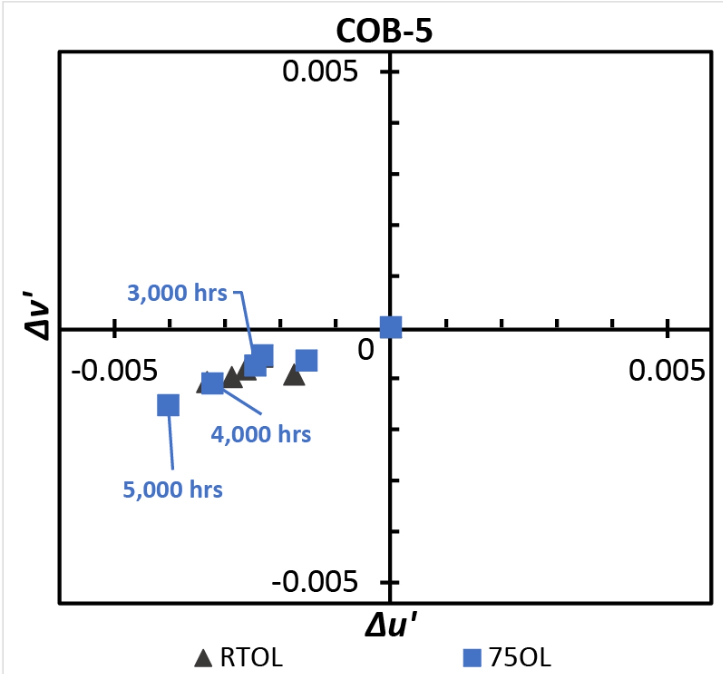

Figure D-5: Chromaticity shift diagram for Product COB-5 during RTOL and 75OL tests.

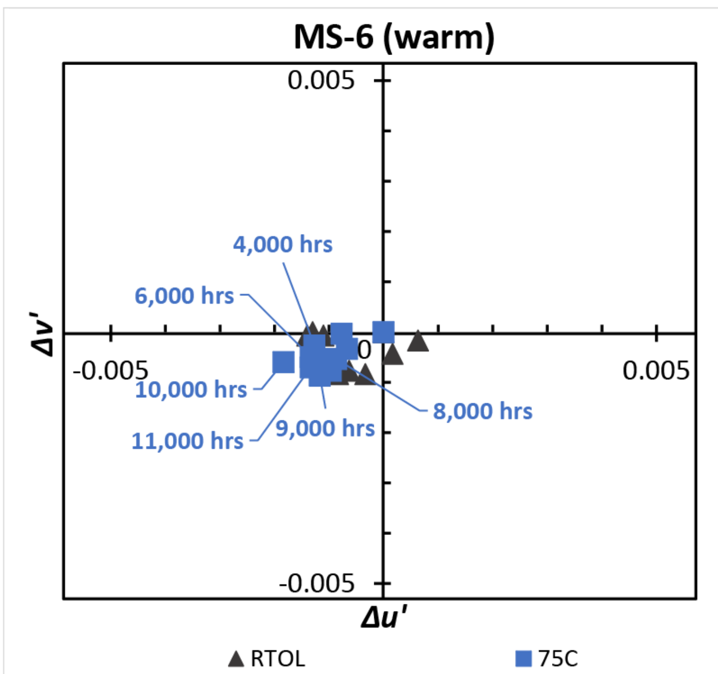

Figure D-6: Chromaticity shift diagram for Product MS-6 (warm) during RTOL and 75OL tests.

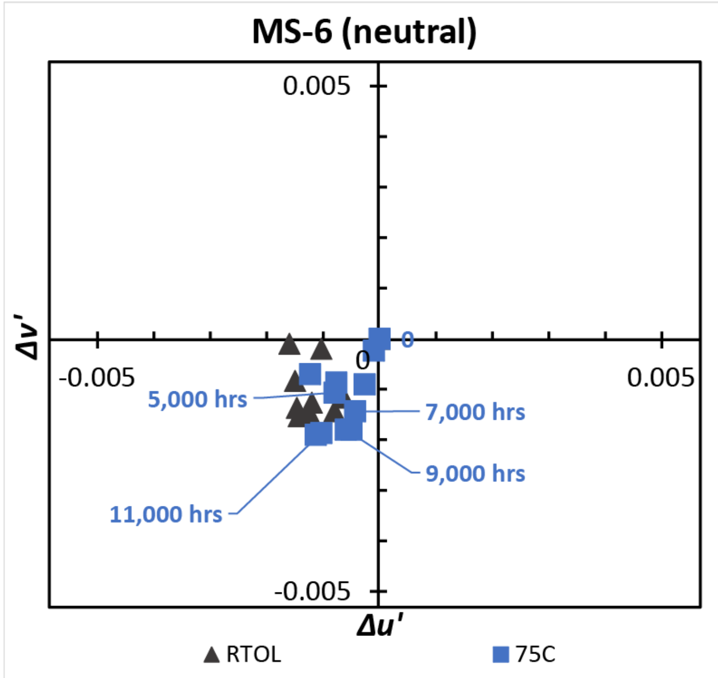

Figure D-7: Chromaticity shift diagram for Product MS-6 (neutral) during RTOL and 75OL tests.

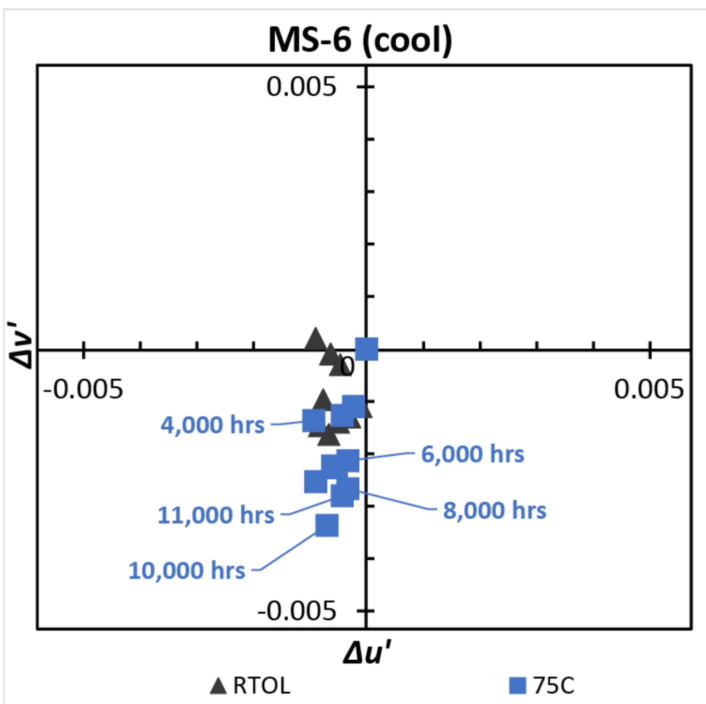

Figure D-8: Chromaticity shift diagram for Product MS-6 (cool) during RTOL and 75OL tests.

(This page intentionally left blank)

U.S. DEPARTMENT OF ENERGY

Office of ENERGY EFFICIENCY & RENEWABLE ENERGY

For more information, visit:
energy.gov/eere/ssl

DOE/EE-2479 ▪ September 2021